



저작자표시-비영리-변경금지 2.0 대한민국

이용자는 아래의 조건을 따르는 경우에 한하여 자유롭게

- 이 저작물을 복제, 배포, 전송, 전시, 공연 및 방송할 수 있습니다.

다음과 같은 조건을 따라야 합니다:



저작자표시. 귀하는 원저작자를 표시하여야 합니다.



비영리. 귀하는 이 저작물을 영리 목적으로 이용할 수 없습니다.



변경금지. 귀하는 이 저작물을 개작, 변형 또는 가공할 수 없습니다.

- 귀하는, 이 저작물의 재이용이나 배포의 경우, 이 저작물에 적용된 이용허락조건을 명확하게 나타내어야 합니다.
- 저작권자로부터 별도의 허가를 받으면 이러한 조건들은 적용되지 않습니다.

저작권법에 따른 이용자의 권리는 위의 내용에 의하여 영향을 받지 않습니다.

이것은 [이용허락규약\(Legal Code\)](#)을 이해하기 쉽게 요약한 것입니다.

[Disclaimer](#)

Master Thesis

Study on the Design, Implementation and Calibration
of 3D Laser Scanner

3D 레이저 스캐너의 설계, 제작 및 캘리브레이션에 관한 연구

The Graduate School
of the University of Ulsan
Department of Mechanical Engineering

Ha Van Tung

Study on the Design, Implementation and Calibration
of 3D Laser Scanner

Supervisor: Byung-Ryong Lee

A Thesis

Submitted to

The Graduate School of the University of Ulsan

In partial Fulfillment of the Requirements

For the Degree of

Master of Science

by

Ha Van Tung

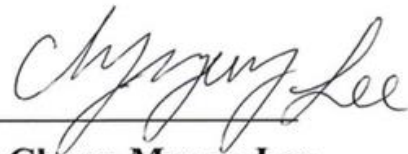
Department of Mechanical Engineering

Ulsan, Korea

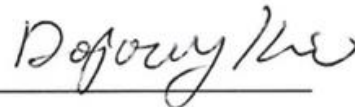
May 2022

Study on the Design, Implementation and Calibration
of 3D Laser Scanner

This certifies that the thesis of Ha Van Tung is approved



Committee Chair Professor Chang-Myung Lee



Committee Member Professor Do-Joong Kim



Committee Member Professor Byung-Ryong Lee

Department of Mechanical Engineering

Ulsan, Korea

May 2022

Acknowledgement

This dissertation is a product of research conducted in Intelligent Control and Mechatronics Lab. (IML), School of Mechanical and Automotive Engineering, University of Ulsan, South Korea.

I would like to express my sincerest thanks to Professor Byung-Ryong Lee, my supervisor, for his effective guidance and support. His expertise and insightful academic advice are my enthusiastic encouragement and thoughtful guidance throughout the study. It was my great honor to be Professor Lee's student.

I would like to express my thankfulness to committee members: Professor Jang-Myung Lee, and Professor Do-Jung Kim for evaluation and their beneficial suggestions.

I would like to thank Dr. Huu-Cuong Nguyen for giving me an opportunity to be a graduate student at University of Ulsan. I would like to send my special thanks to him, Dr. Van-Phu Do, and Dr. Chi-Tho Cao at the University of Ulsan who bringing me a lot of knowledge and understanding in all aspects.

Many thanks to my friend here in Ulsan, their meaningful support and sense of humor was mean a lot to me. Without them, I would have had many stressful moments.

Finally, I would like to thank my family. Their support and encouragement are always mean to me.

Ulsan, Korean. May 2022.

Van-Tung Ha

Abstract

This research develops a 3D scanning system with a line laser projector, a camera, and a turntable for movable objects reconstruction. A detail process will be given to give an overview of how to build a 3D laser-based scanning system, from designing to calibration, and 3D reconstruction. To obtain the 3D information of the scanning object, all the elements have to be calibrated. Our system has three elements including camera, line laser, and the motor or turntable. Therefore, we propose two calibrations process. Because the camera is the only receiver device which can 'see' the other devices, we choose camera as the 'standard device' which the other devices information will transform to camera coordinate system. Therefore, we propose three calibration steps as: camera itself calibration, camera-laser calibration, and camera-motor calibration. With the prevalence of information nowadays, the camera calibration, and camera-laser calibration are well-know, therefore, our thesis will focus on camera-motor calibration which is also our contribution.

In our novel calibration method for 1-axis rotating mechanism, we will focus on 2 parameters, which are virtual rotation axis, and point on rotation axis. The rotation axis represents for the rotation transformation of motion, and the point on rotation axis represents for translation relationship. The calibration requires calibration board. At every angle of the motion, the camera acquires the calibration pattern image to determine the origin coordinate of the camera coordinate system. The trajectory of them is then estimated as a spatial circular to find its center point, known as point on rotation axis. The normal vector of the plane created by the camera origins is used as the virtual rotation axis. The whole real scanning system was tested by applying a comprehensive checking method to the scanning results. From the planarity testing experiment, it was shown that the average of the planarity is 0.3379mm. The accuracy test was performed with the calibration block showing that its maximum error is 0.0637 mm, and its average in 15 testing time is 0.0153 mm. The scanning quality is also checked by scanning different shape objects.

Keyword: 3D reconstruction, turntable, triangulation.

TABLE OF CONTENTS

Acknowledgement.....	1
Abstract	2
LIST OF FIGURES.....	5
LIST OF TABLES	7
1. Introduction	8
1.1 Literature review	8
1.1.1 3D scanning system [1]	8
1.1.2. Laser-vision systems with principle of rotation	9
1.1.3 Application	11
1.2. The Scope of Study	12
1.3. Outlines	12
2. Background theory	13
2.1. Camera model and camera calibration.....	13
2.2. Laser vision technology	15
2.2.1. Laser triangulation.....	15
2.2.2. Laser-camera calibration	16
2.3. 3D circle estimation	18
3. Method	20
3.1. Overall System.....	20
3.1.1. Mechanical and Hardware	20
3.1.2. Processing of the scanning system	21
3.2. Laser detects algorithms	22
3.3. Calibration method.....	22
3.3.1. Construction on the target coordinate system	22

3.3.2. Camera calibration.....	23
3.3.3. Camera-laser calibration.....	23
3.3.4. Camera-motor calibration.....	24
3.4. 3D surface reconstruction	29
3.4.1. Introduction [6].....	29
3.4.2. Data collection and preprocessing.....	29
3.4.3. Merging the point cloud dataset into a single point cloud.....	30
3.4.4. Removing noise and background	31
4. Experiments and results	34
4.1. Calibration experiments	34
4.2. Result	36
4.2.1. Planarity of the plane.....	36
4.2.2. Accuracy check.....	38
4.2.3. Scanning quality check.....	40
5. Conclusion, limitation, and future work.....	42
Reference.....	43

LIST OF FIGURES

Figure 1.1. Overall 3D scanning technique.....	9
Figure 1.2. Laser scanning system with a rotary mechanism.....	10
Figure 1.3. Laser-vision system [6].....	11
Figure 2.1. Pinhole camera model.....	13
Figure 2.2. Pinhole camera model with image plane.	13
Figure 2.3. Radial distortion. a) Barreal distortion; b) Pincushion distortion.	14
Figure 2.4. Laser-vision triangulation principle [25].	15
Figure 2.5. Triangulation by line-plane intersection [25].	15
Figure 2.6. Laser plane and camera coordinate system.....	17
Figure 2.7. 3D circle estimation. (a) Set of points of a circle in 3D space; (b) The procedure for estimating the center of a circle in space.	18
Figure 3.1. Relationship between camera and laser position.	20
Figure 3.2. System's device.	21
Figure 3.3. Laser scanning with turntable system.	21
Figure 3.4. (a) Flow chart of the calibration process; (b) Flow chart of the scanning process.	22
Figure 3.5. (a) Capture of calibration board; (b) Coordinate system of calibration board.....	23
Figure 3.6. Process of camera-laser calibration.	24
Figure 3.7. a) Virtual rotation axis defines; b) Camera coordinate systems at different times with the point of view is lie in the rotation axis.	25
Figure 3.8. Relationship between the laser point in the corresponding coordinate system to the absolute coordinate system.	26
Figure 3.9. Pipeline of the camera-motor rotation axis calibration process.....	28
Figure 3.10. Triangulation based laser camera scanning [6].....	30

Figure 3.11. (a) Laser profile without transformation to ACS; (b) Laser profile after transform to ACS.	31
Figure 3.12. (a) Concept of scenery background; (b) Noise from scene; (c) Scanning result with noise from background in (a); (d) Scanning result after removing noise; (e) Scanning result with noise from scene in (b).	32
Figure 3.13. (a) ROI method for removing noise from the scene; (b) Distance of interest method to remove unwanted laser stripe.	33
Figure 3.14. Scanning result after removing noise.	33
Figure 4.1. (a) The designing of camera-laser platform. (b) Camera-laser platform.	34
Figure 4.2. Laser plane in different viewpoint.	35
Figure 4.3. (a) The camera origin trajectory; (b) The camera origin trajectory and its estimated center points.	35
Figure 4.4. a) Definition of the plane constraints considering planarity [33]; b) Illustration of the ideal plane, real plane, and planarity of a plane; c) Result of our ideal plane and estimated plane.	36
Figure 4.5. (a) Set up of experiment for planarity check; (b) Scanning result of the planarity check.	37
Figure 4.6. (a) Calibration block; (b) Dimension of the calibration block; (c) Scanned result of calibration block; (d) Illustration of the way to measure the distance between two planes.	39
Figure 4.7. Two-planes distance checking with calibration block.	39
Figure 4.8. Scanning workspace for quality check and its scanning result.	41
Figure 4.9. (a) Real human statue used for quality check; (b) Scanning result of the quality check.	41

LIST OF TABLES

Table 1. Camera and camera-laser calibration results.....	35
Table 2. Camera-motor calibration results	36
Table 3. Planarity result of the scanned calibration board	38
Table 4. The average and the error of the distance between the two planes of the calibration block with different scanning results.....	40

1. Introduction

Three-dimensional (3D) scanner is a discipline that studies how to reconstruct, interpret and understand a 3D scene or a real object from its two-dimensional (2D) image. During the last decades, 3D scanner systems have been widely used in industry, autonomous vehicles, digital entertainment, and many aspects of our daily life. In this dissertation, we introduce our development of 3D scanner system using a camera, line laser projector, and a turntable for 3D reconstruction.

1.1 Literature review

1.1.1 3D scanning system [1]

With the development of computer vision technology, the 3D computer vision has become popular [2–5]. 3D computer vision is a process of regeneration, processing, and application of 3D information of scene which is captured by image sensors using the 2D images [6]. This 3D information is call digital 3D models. Applications based on the 3D model are growing more and more popular due to the increasing of availability of 3D graphic devices and the decreasing cost of the computational power. The popularity of 3D digital models arises from the possibility of processing them digitally: their visualization and modification and the display in real time of the interaction of the model with other digital objects are among the key advantages of digital models with respect to physical copies. Some typical applications that use of the 3D models such as archeology, architecture; fashion design, production; medical applications; entertainment industry, etc.

The acquisition process of the surface geometry of a real object and of its visual appearance is called 3D scanning and the system used to this aim is called 3D scanner. The 3D scanning system use, mainly, two acquisition techniques. The first one is the contact technique which based on the interaction between a sensor and the surface of the object. The other one is the non-contact technique which is based on the interaction between a radiation (sound, light), and the surface of the object [6].

In this thesis, we aim to study the non-contact technique which uses an optical technique. The advantage of this technique is that we can perform the reconstructing process without any physically touching to the scanning object. This ability helps us develop the numerous of application in the fragile objects, hard-to-reach objects, or complex shape one, with the high collecting speed data. Moreover, this kind of system can be built with a low budget. The none-contact 3D scanning system can be divided into two types based on its devices or source of the radiation: passive or active system. The overall of 3D scanning technique is shown in Figure 1.1.

Passive scanning system used the radiation reflected by the objects surface, and collect the information from different viewing side, or lens arrangements, to perform the reconstruction. Such system usually uses charge-coupled device (CCD) sensors employed by commercial digital camera. This kind of system can be cheap as they do not require any other hardware.

However, passive method has low accuracy, and require a large computation effort to produce a set of 3D data over the surface.

Active scanning system is a combination of radiation source devices and receiver devices. The radiation source devices will project radiation such as visible light or pattern to the scanned surface, and the receiver devices will capture the image of the object with pattern. Depend on the using technique, one or more images will be collected. By analysis these images, the position of the projected pattern over the surface can be obtained. This thesis focuses on the active technique called active triangulation technique, which based on the triangulation relationship between the source devices and its corresponding receiver devices.

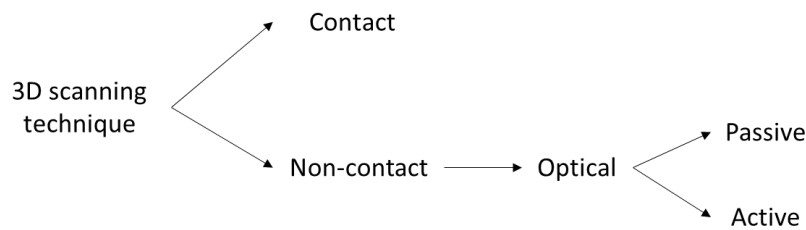


Figure 1.1. Overall 3D scanning technique.

1.1.2. Laser-vision systems with principle of rotation

Overview

In the active triangulation system, the scene is illuminated by a coherent or incoherent light pattern from one direction and viewed from another. These systems primarily different pattern used (single laser spot, laser line, laser grid, etc.) and for the scanning method (motion of the object or scanner). When the scene is lighted up by a laser projector and its lighted up part is captured by a camera, we can understand this kind of system as a laser-vision scanning system or laser scanning system. Laser scanning is the most popular because of its advantages: simple structure, easy to use, wide measurement range with high measurement efficiency, and it has great potential in the field of technical metrology [7–9].

Most of the cheap-priced 3D scanner has a limited scanned area, a lot of technology was proposed to improve that limit when adding a rotary mechanism [10–12], or the combination of a rotating laser and a static stereo camera [13]. Therefore, many algorithms with different architectures and measurement methods have been proposed. In general, the scanning system with the principle of rotation is divided into two main categories: the axis of rotation located in the field of view of the camera and the axis of rotation outside the field of view of the camera. Depending on the rotation principle, different calibration principles are proposed. For the first case where the rotation axis is in the camera viewing field, using a system with a multi-view stereo camera, Huajun Cai [14] presented a multi-camera calibration algorithm using a turntable and a calibration plate. Livio Bisogni [15] proposed a two-axis rotary table system, using one checkerboard with several images in different poses to determine two axes' information. When the rotation axis is located outside the camera viewing area, Laksono Kurnianggoro [16]

developed a rotating laser range finder, using the calibration plate based on a point-plane constraint to form a transformation matrix including rotation axis and rotation radius information. Jaeho Lee developed a model with a rotating line laser and a fixed camera with a large viewing field using a special calibration board to determine the changing of the laser plane when it rotates. Niu [17] used two checkerboards and another camera to find the relationship between the orientation of a camera fixed on a rotation axis, Zhihao Zhu [18] used one calibration board for finding the transformation matrix.

This thesis develops a laser scanning system with a rotary mechanism, in case the rotation axis is in the camera viewing field as, shown in Figure 1.2.

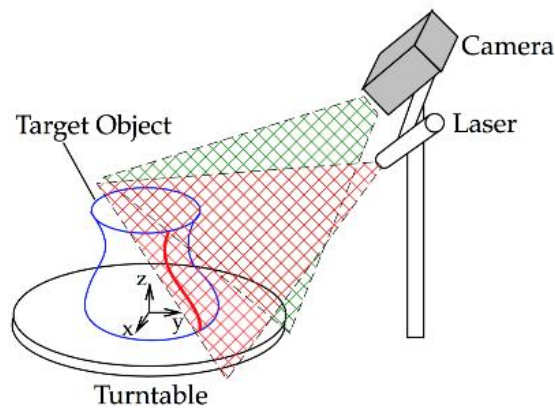


Figure 1.1. Laser scanning system with a rotary mechanism.

Working principle of laser scanning systems with principle of rotation

We divide the scanning process of the laser scanning system into two phases: image acquisition and motor rotation. Therefore, scanning techniques are also divided into two main techniques: techniques to reconstruct objects from a fixed frame or the laser triangulation technique, and techniques to combine point clouds in each frame of a motor angle coordinate system into an absolute coordinate system.

The laser triangulation method is a model of a stereo system that determines the location of a point which is the intersection of the laser line pattern and the camera sensor. Figure 1.3 illustrate an example of a single spot laser-vision system, the orientation and position of laser source and camera are typical known. The line between the laser spot and camera center point can be computed, line $l1$. By combined $l1$ with the known in advance of the direction of the laser $l2$, the 3D position of the spot on the object can be computed as the intersection between $l1$ and $l2$ based on the triangulation relationship.

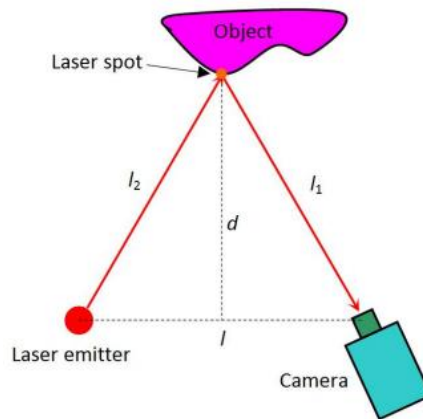


Figure 1.3. Laser-vision system [6].

When the laser projector project the more complex patterns like lines or grids laser, more than one point per frame can be captured. In this study, we used line pattern or line laser projector. The laser line is described as a 3D plane, the camera captures the laser stripe resulting from the intersection of laser plane and the object surface. Then, instead of a single laser spot, we get a multi-laser spot or line, for any laser spot, the corresponding 3D point on the object surface can be found, the detail will be discussed in section.

Rotation motion is the motor's rotation, which has its corresponding rotation axis coincident with the motor rotation axis. In our system, camera position and the motor position are not change, therefore, the rotation axis is also not change in the camera coordinate system. In order for the laser line image cover the large area in the camera field of view while rotating, the camera origin, and the rotation axis does not lie in the same line. Therefore, the relationship between the camera coordinate systems at different times is not only the rotation transformation. A translation relationship between them should be added to realize multi-frame splicing. In our system, the laser-camera platform is placed at a distance from the rotation axis to make sure that the camera can see an enough object area. In this study, we perform the combination technique by using the two-parameter using the camera-motor calibration called rotation axis identification which will be describe in section 3.

A rotation axis identification process is proposed to solve the problem because it is not changed during the rotation motion. In this case, we defined the rotation axis as the normal vector of a plane in which the camera origin moves, and a point on the axis of rotation as the center of a spatial circle that is the trajectory of the origin of the camera coordinate system, from here, we call it as the center point. A calibration method is performed to extract two parameters that are defined according to the camera coordinate system. Using these parameters, we can obtain the transformation matrix between any camera's pose to a reference pose that is useful for 3D reconstruction.

1.1.3 Application

This section summarizes the reviewing of some applications based on the laser-vision technologies which is related to our study. Applications of laser scanner in industry

manufacturing, quality product inspection, large-scale object measurement, and 3D point cloud data acquisition.

In Precise 3D Inspection and Assembly [19], laser-vision is used as an eye of arm robot call hand-eye robot, which is used to determine the position of the assembling part. Measurement processing for inspection plays a vital role in manufacturing to guarantee the quality of products. Contactless and nondestructive measurement methods for large-scale or small-scale objects have been studied based on stereo vision and laser vision techniques [20]. For 3D model reconstruction applications, 3D point cloud data acquisition systems based on stereo vision and laser vision were also developed [21,22].

In the last three decades, there are many studies laser vision technologies. These research results could be applied in many fields such as industrial manufacturing, quality inspection, measurement, and 3D point cloud data collection.

1.2. The Scope of Study

The purpose of this dissertation is to provide an overview of the laser 3D scanner system. We implement a detail process in designing, calibration, and reconstruction a line laser scanner with turntable system.

Firstly, we briefly review some basic knowledge and principles of 3D computer vision, such as camera pinhole model, calibration, laser-vision triangulation, and technology, etc. Concurrently, we also reviewed some related works about laser vision technologies.

Subsequently, we build a scanner system for 3D surface reconstruction. The complete 3D surface of real objects was automatically reconstructed using laser-vision technology. The proposed system is a combination of a laser-camera system and a rotatable mechanism.

In addition, a method for checking scanning quality and scanning accuracy was proposed.

1.3. Outlines

The following section will introduce some basic knowledge about camera model, camera calibration, laser vision technology, and geometry knowledge which will be used in this study. Section 3 will implement the detail methods including designing system, and calibration process. The experiments and results will be described in section 4, where all the testing and checking our real system are performed. Section 5 draws the conclusion and discuss ideas of future work.

2. Background theory

In this section, we would like to show some vision, laser vision technology, and mathematic background which were use in our study.

2.1. Camera model and camera calibration

A camera is a device that records lights coming from the scene and saves them in images. These images may be photographs or consecutive photographs (video). The camera model describes the mathematical relationship between the 3D coordinates of a point in the scene from which the light comes from and the 2D coordinates of its projection onto image plane. The ideal camera model is known as the pinhole camera. Figure 2.1 illustrates the pinhole camera model. In the pinhole camera model, we assume that only light coming through the pinhole can reach the image plane. Light from the scene or object passes through the aperture and projects an inverted image on the image plane. Or each point on the object combines with corresponding points on the image to create a straight line through the pinhole.

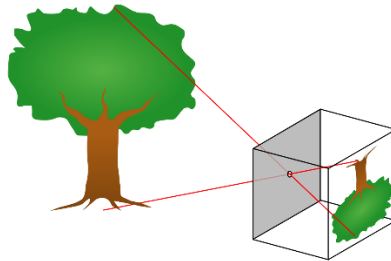


Figure 2.1. Pinhole camera model.

Figure 2.2 is the pinhole camera model with the image plane uv , the principal point (c_x, c_y) , and the focal length f is defined as the distance between the optical center F_c and the image plane. These parameters are known as camera parameters.

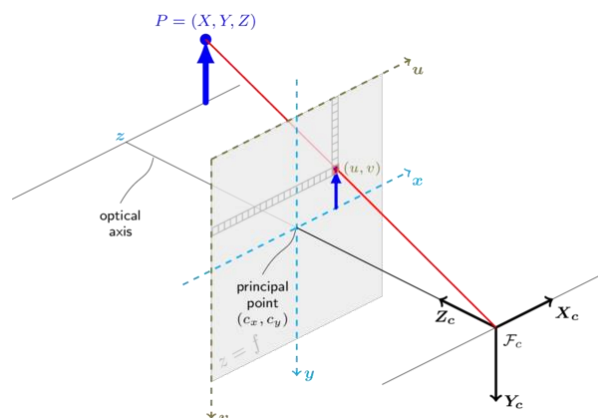


Figure 2.2. Pinhole camera model with image plane.

Camera calibration is a computational and experimental method to find out camera's parameters to reproduce the 3D model of a scene, a particular object, or measure the size and

the distance to the object using image captured by the camera. The calculations are performed in the camera pinhole model.

In actually, the real camera usually uses lenses with finite aperture, especially for low-end or wide-angle cameras. Lens distortion also arises from imperfect lens design and manufacturing, as well as camera assembly, Figure 2.3 shows some popular type of camera distortion can be caused by different lens. Figure 2.3 a illustrate barrel distortion, this distortion is the non-linearly increased of image magnification with distance from the optical axis. In the pincushion distortion shown in Figure 2.3 b, image magnification decreases non-linearly with the distance from the axis. In fact, there exists the pincushion distortion of the camera lens as define as the misalignment of optical elements a compound lens. This distortion is shown in the Figure 2.2 as the principal point (c_x, c_y) .

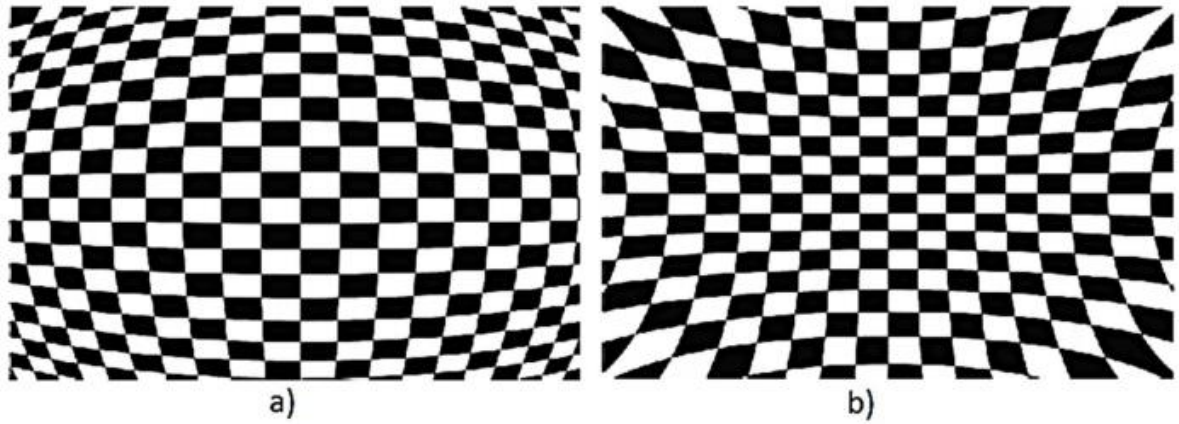


Figure 2.3. Radial distortion. a) Barreal distortion; b) Pincushion distortion.

The most common representation of radial and tangential distortion is Brown's distortion model [23,24], which represents the distorted image coordinate as:

$$r = \begin{pmatrix} r_x \\ r_y \end{pmatrix} = x_u - cc; \quad r = |r| \quad (1)$$

$$x_d = (1 + k_1 r^2 + k_2 r^4 + k_3 r^6) x_u + \begin{pmatrix} 2k_4 r_x r_y + k_5 (r^2 + 2r_x^2) \\ k_5 (r^2 + 2r_y^2) + 2k_4 r_x r_y \end{pmatrix} \quad (2)$$

where x_u, x_d are the undistorted and distorted point coordinates, $k(1,2,3,4,5)$ the distortion coefficients (first three radial and the rest tangential), and cc the principal point. Therefore, a point in 3D space, its corresponding point in image plane, and the camera's optical center are not collinear. When these parameters are found, images can be corrected for distortion by warping by a function that map the image points from the distorted coordinate system to undistorted coordinate system.

Therefore, when performing the camera calibration, we need to determine more the distortion parameters. These all parameters called intrinsic parameters.

2.2. Laser vision technology

2.2.1. Laser triangulation

Laser triangulation is a technique that perform the reconstruction using the triangulation. In fact, it is common for the laser projector projected illuminate patterns (point or line) to the scene or object. In case of line laser projector, the illuminate patterns are actually a plane of light (laser plane), and the lighted up part on the object is the intersection between the laser plane and the object surface. When the laser is a spot laser, the illuminate patterns is a ray of light, and the visible point we saw on the object surface is the intersection between the ray of light and the object surface. In this study, we will consider only the line laser projector case.

When the intersection of a ray of light with the object being scanned can be considered as a single illuminated point, the intersection of a laser plane with the object generally contains many illuminates curved segments as show in Figure 2.4. Each of these segments is a combination of many lighted up point or laser spots. Every single laser spot, which is visible to the camera, can define a camera ray.

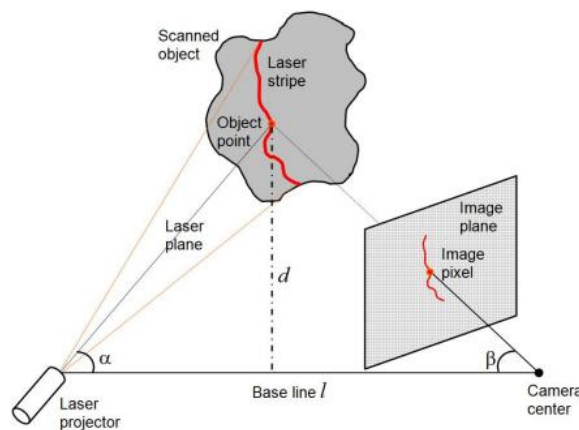


Figure 2.4. Laser-vision triangulation principle [25].

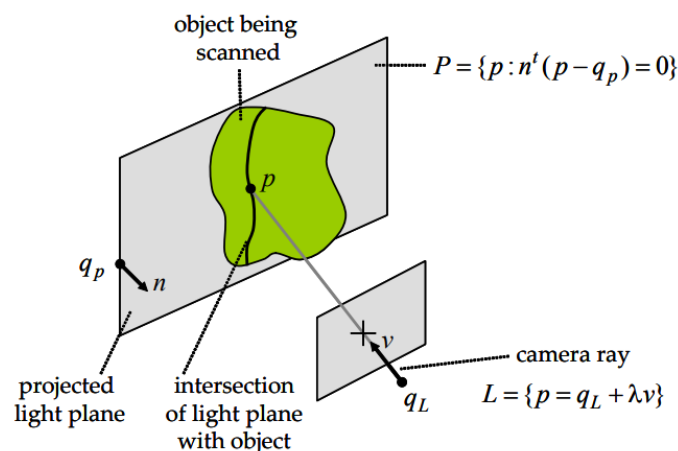


Figure 2.5. Triangulation by line-plane intersection [25].

For now, we assume that the location and orientation of camera and laser are show in Figure 2.5. In additional, we assume that the laser plane is display as the equation below:

$$P = \{p: n^t(p - q_p) = 0\} \quad (3)$$

Where p is any point on the laser plane, q_p is the known-coordinate on the laser plane, and n is the normal vector of the laser plane. Furthermore, we assume that the laser spot p is the unknow points lie on the intersection line. Called v is the vector from the optical center of the camera to the laser spot, with λ is an arbitrary, the camera ray now can be written as equation

$$L = \{p = q_L + \lambda v\} \quad (4)$$

Point p now can be understood as the intersection of laser plane P and camera ray L . In case of the plane and the ray parallel, we will have that the dot product of v and n^t is equal to 0. This case will also happen when the camera ray is contained in the plane P . In the other case, when $n^t v \neq 0$, there is always exactly one point p exist. Since this point belong to the line, it can be written as $p = q_L + \lambda v$, which is λ is an arbitrary value that we need to determine. On the other hand, p is also belongs to the plane P , therefore, the value λ must satisfy the linear equation:

$$n^t(p - q_p) = n^t(q_L + \lambda v - q_p) = 0 \quad (5)$$

Since we remove the parallel case, the λ value will always exist. The geometric interpretation of line-plane intersection is provided in Figure 2.5.

2.2.2. Laser-camera calibration

Camera-laser calibration is a process of specifying the mathematical (6) of the laser plane in the camera coordinate system as show in Figure 2.6. The camera coordinate system is denoted as $\{C\}$, and the originates at the optical center of the camera. Axis Z_c is defined as the viewing direction of the camera along the optical axis. Axis X_c is the same as the horizontal axis of the image. Our work now is to determine laser points in the camera coordinate system. Then, from the collection of that, we can easy estimate the plane equation using least square method.

$$l: Ax + By + Cz + D = 0 \quad (6)$$

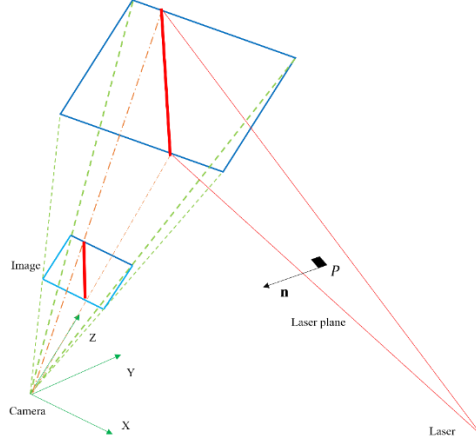


Figure 2.6. Laser plane and camera coordinate system.

- Fitting a plane in 3 dimensions [26]

In our study, we will use least square method to fit a collection of points to a plane equation. Assume that our final equation is $h = a_0x + a_1y + b$, where a_0, a_1, b are scalar values. This define a plane that best fits the collection of points in the sense that the sum of squared error between the h_i and the plane value $a_0x + a_1y + b$ is minimized.

Define the error function:

$$E(a_0, a_1, b) = \sum_{i=1}^m [(a_0x_i + a_1y_i + b) - h_i]^2 \quad (7)$$

This function is a nonnegative and its graph is a hyper paraboloid whose vertex occurs when the gradient satisfies $\nabla E(a_0, a_1, b) = \left(\frac{\partial E}{\partial a_0}, \frac{\partial E}{\partial a_1}, \frac{\partial E}{\partial b} \right) = (0, 0, 0)$. This leads to a system of three linear equations in a_0, a_1 , and b which can be easily solved. Precisely,

$$\begin{bmatrix} \sum_{i=1}^m x_i^2 & \sum_{i=1}^m x_i y_i & \sum_{i=1}^m x_i \\ \sum_{i=1}^m x_i y_i & \sum_{i=1}^m y_i^2 & \sum_{i=1}^m y_i \\ \sum_{i=1}^m x_i & \sum_{i=1}^m y_i & \sum_{i=1}^m 1 \end{bmatrix} \begin{bmatrix} a_0 \\ a_1 \\ b \end{bmatrix} = \begin{bmatrix} \sum_{i=1}^m x_i h_i \\ \sum_{i=1}^m y_i h_i \\ \sum_{i=1}^m h_i \end{bmatrix} \quad (8)$$

We can easily solve the problem using numerical algorithms. If implemented directly, this formulation can lead to an ill-conditioned linear system. To avoid this, we can follow the equation below:

$$\begin{aligned}
\begin{bmatrix} l_{00} & l_{01} & 0 \\ l_{01} & l_{11} & 0 \\ 0 & 0 & m \end{bmatrix} \begin{bmatrix} \bar{a}_0 \\ \bar{a}_1 \\ \bar{b} \end{bmatrix} &= \begin{bmatrix} \sum_{i=1}^m (x_i - \bar{x})^2 & \sum_{i=1}^m (x_i - \bar{x})(y_i - \bar{y}) & 0 \\ \sum_{i=1}^m (x_i - \bar{x})(y_i - \bar{y}) & \sum_{i=1}^m (y_i - \bar{y})^2 & 0 \\ 0 & 0 & m \end{bmatrix} \begin{bmatrix} \bar{a}_0 \\ \bar{a}_1 \\ \bar{b} \end{bmatrix} \\
&= \begin{bmatrix} \sum_{i=1}^m (h_i - \bar{h})(x_i - \bar{x}) \\ \sum_{i=1}^m (h_i - \bar{h})(y_i - \bar{y}) \\ 0 \end{bmatrix} = \begin{bmatrix} r_0 \\ r_1 \\ 0 \end{bmatrix}
\end{aligned} \tag{9}$$

Then we can have the solution:

$$\bar{a}_0 = \frac{l_{11}r_0 - l_{01}r_1}{l_{00}l_{11} - l_{01}^2}, \bar{a}_1 = \frac{l_{00}r_1 - l_{01}r_0}{l_{00}l_{11} - l_{01}^2}, \bar{b} = 0 \tag{10}$$

In term of the original inputs, $a_0 = \bar{a}_0, a_1 = \bar{a}_1, b = \bar{h} - \bar{a}_0\bar{x} - \bar{a}_1\bar{y}$.

2.3. 3D circle estimation

Call $\{O\}$ is a set of 3D points of a circle in the 3D space as shown in Figure 2.7 (a). Call p is the plane contain the circle, every pair of point $\{O_i, O_{i+1}\}$ will form a line segment on plane p . Call $\{L\}$ is a set of line segments which formed from any two points on the circle. We can say that the perpendicular bisector of every element on $\{L\}$ always pass through the center of the 3D circle. Therefore, using the coordinates of at least 3 points on the arc, we can easily find the center of the circle and its corresponding radius, as shown in Figure 2.7 (b).

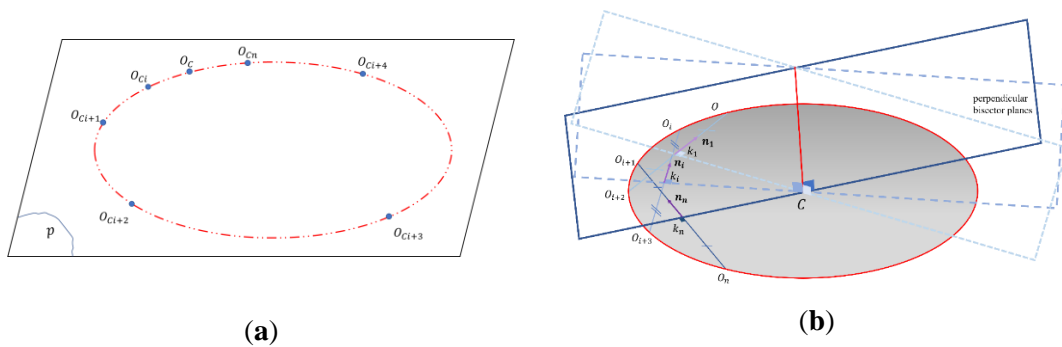


Figure 2.7. 3D circle estimation. (a) Set of points of a circle in 3D space; (b) The procedure for estimating the center of a circle in space.

In fact, a line segment in three-dimensional space has infinitely many perpendicular bisectors lying on the orthogonal plane, so we need to determine the one containing the center of the circle. With each line segment $O_i O_{i+1}$ in the set $\{L\}$, we define an orthogonal plane with the normal vector $n_i = O_i O_{i+1}$, and a point on plane as a center point of line segment. Call $\{S\}$

as the set of orthogonal planes of $\{L\}$. The perpendicular bisector containing the center point now is defined as the intersection between the perpendicular bisector plane of the line segment and the plane containing the circle, as illustrate in Figure 2.7 b. As the result, we call $\{B\}$ is the set of the perpendicular bisector that contains the center point of the circle. Call C is the center point of the circle, we can find C by finding the intersection of lines from $\{B\}$.

3. Method

This section will describe the steps of designing a turntable laser scanner in detail, from designing the hardware, detecting laser, and calibration method.

3.1. Overall System

3.1.1. Mechanical and Hardware

There are three main elements in our system: a line laser projector that fix with a camera in a platform, and a motor with turntable. The line laser-camera platform is designed follow the Figure 3.1. With the constant value d_2 , known as the distance between camera origin and the laser, the angle value α is now dependent on the distance d_1 between the rotation center and the laser. Therefore, α can be calculated as:

$$\alpha = \tan^{-1} \frac{d_1}{d_2} \quad (11)$$

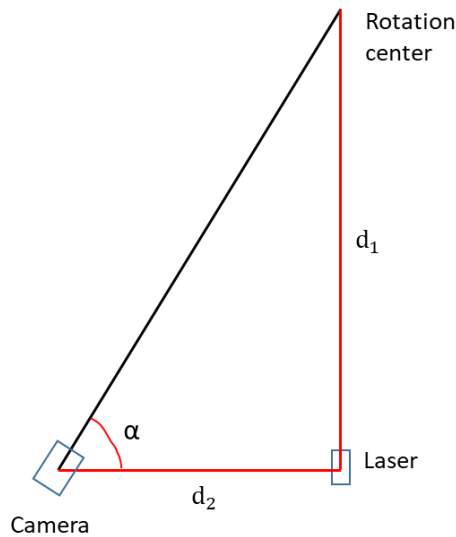


Figure 2.1. Relationship between camera and laser position.

Shown in Figure 3.2. We use laser M-14A650-5-L, and a Basler camera (acA1440-220um) with 4mm focal lens. We design a platform that fix the laser, camera, and the turntable together. We use A50K-M566-R10 with the resolution of 0.36 degree/step. For motor control, we used Arduino Uno and the motor controller MD5-HD14 which can adjust the motor resolution. The final system is shown in Figure 3.3.



Figure 3.2. System's device.

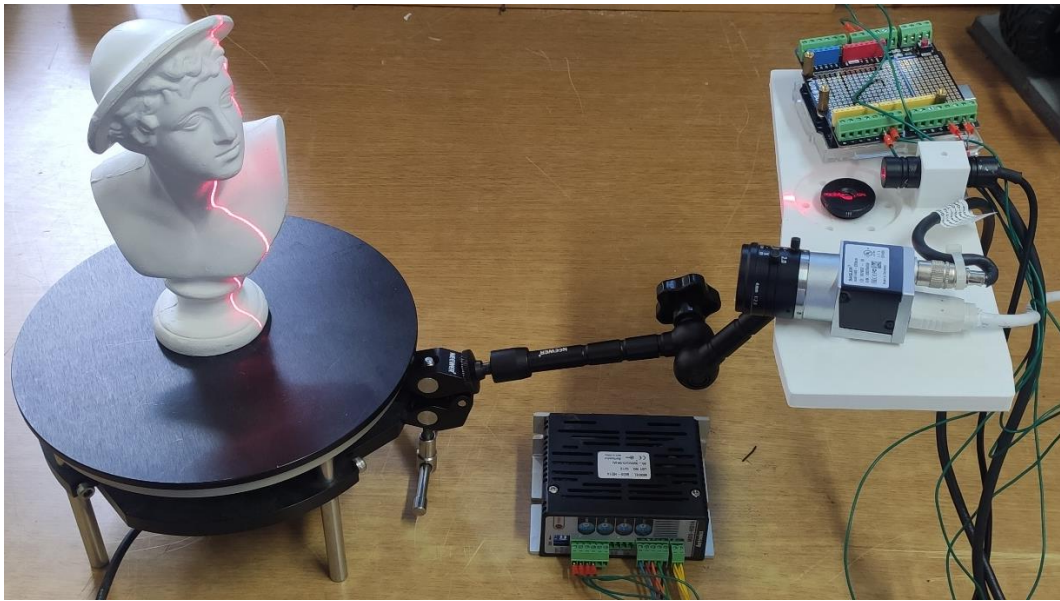


Figure 3.3. Laser scanning with turntable system.

3.1.2. Processing of the scanning system

Three processes were performed to collect 3D data from 2D image data as show in Figure 3.4 (a), and (b). Because our scan is made up from three main components, we specified the transformation interdependence of the camera and the other two devices via calibration.

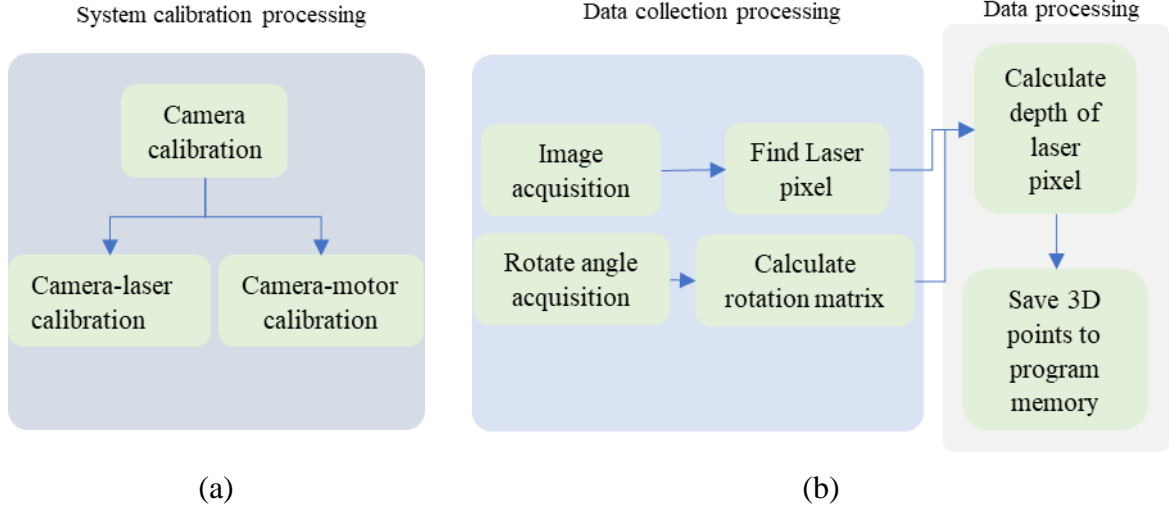


Figure 3.4. (a) Flow chart of the calibration process; (b) Flow chart of the scanning process.

At every angle of the motor, the laser will illuminate at a corresponding position on the surface of the scanning object. Therefore, a sequence of adjacent consecutive angular positions will give a sequence of corresponding laser line images consecutively on the surface of the scanning object. By extracting the coordinates of the laser lines from the corresponding image, combined with the calibration data information and the angular value of the motor, we can determine the coordinate value in the 3D space of the respective object. Using the obtained data, we can conduct a simulation or save it in computer memory.

3.2. Laser detects algorithms

Extracting laser line or laser peak is the essential step which will affect the result of reconstruction. Many algorithms were proposed [27] with their advantages and disadvantages. In this dissertation, we used Blais and Rioux Detectors (BR4) [28] because it has a good performance for the stripe widths with Gaussian width parameters larger than 2 pixels and low error.

3.3. Calibration method

We divide the scanning process into two phases: image acquisition, and motor rotation. Therefore, the scanning techniques are also divided into two main techniques: techniques to reconstruct objects from a fixed frame or the laser triangulation technique, and techniques to combine point clouds in each frame of a motor angle coordinate system into an absolute coordinate system. The laser triangulation method is a model of a stereo system that determines the location of a point which is the intersection of the laser line pattern and the camera sensor.

3.3.1. Construction on the target coordinate system

Figure 3.5 is a capture of coplanar calibration board with 121 circular features (11 rows and 11 columns) that is used in this study. The circular feature in the board appears as the elliptical shape in the image. The feature points for the calibration process are defined as the center of the circles. The center point of the middle circle is defined as the origin of the target coordinate

system. There are 4 larger circles that are main processes are located around the middle center to locate the 3 axes of the target coordinate system. The final target coordinate system is shown in Figure 3.5 (b).

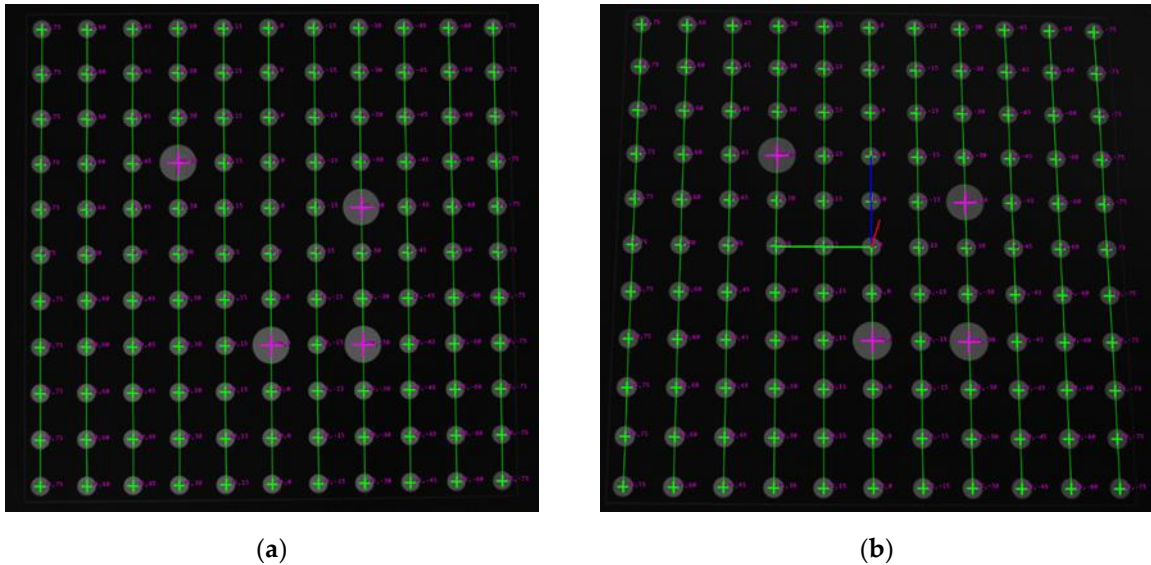


Figure 3.5. (a) Capture of calibration board; (b) Coordinate system of calibration board.

3.3.2. Camera calibration

Camera calibration is a prime step in 3D reconstruction to extract metric information from 2D image. The purpose of camera calibration is to determine the intrinsic parameters that maps the 3D points in the world coordinate system to the 2D image coordinates. There are many algorithms was proposed for camera calibration [29]. Zhang’s method is the most popular because of its high precision and easy operation [30].

This study will use Zhang’s method and OpenCV C++ to perform camera calibration.

3.3.3. Camera-laser calibration

As mentioned before, we need to determine the laser plane equation in the camera coordinate system. We can achieve this purpose through finding the coordinate of at least three points on laser plane in the camera coordinate system. Because the laser line also belongs to the camera field of view, we can find these points using the image of the laser line or the pixel coordinate of the laser line using the laser detects algorithm we mentioned before.

Now, we have the laser line coordinate in the pixel coordinate system, which is needed to convert to the camera coordinate system. The relationship between pixel coordinate system, world coordinate system, and camera coordinate system is shown in Figure 2.6, with its corresponding equation as shown in equation (6). From now, if we want to perform the conversion, one more transformation matrix between the camera coordinate and world coordinate system needs to be determined. The calibration board is used to obtain transformation information between the camera coordinate system and the world coordinate system.

In summary, at each laser line pose, we need to acquire two images [31], one containing the laser line, another holding the calibration features. The process of the camera-laser calibration is shown in Figure 3.6. The coordinates of the laser points in the calibration board are obtained using the homography between the feature points of the calibration board and its image. The transformation relationship is obtained using the perspective-n-point algorithm. By combining the coordinate of the laser points and transformation information, we can obtain the coordinate of the laser points in the camera coordinate system. Using the least-square method to fit these points to the plane equation, we can easily determine the camera-laser calibration information.

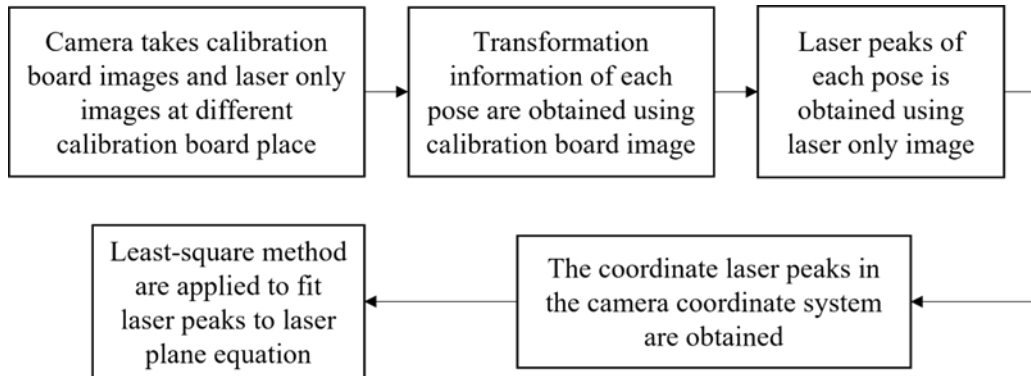


Figure 3.6. Process of camera-laser calibration.

3.3.4. Camera-motor calibration

Overview

Camera-motor calibration is a process of determining the transformation relationship between the camera and motor motion. Based on the camera-laser calibration, we already determine laser stripe in the camera coordinate system. Without loss of generality, we will also find the transformation matrix between the motor angle coordinate system and the camera coordinate system, as known as finding rotation axis identification.

For the rotation axis identification, we need to define the rotation axis and the point on the rotation axis. As the motor rotates, the turntable and the scanning object on the turntable will be move together with the motor. From there, we define the rotation axis u as a virtual axis, which perpendicular with any plane forming by the orbit of any point rotates with the motor, as shown in Figure 3.7 (a). Considering any point on the turntable, when the motor rotates, the orbit of that point is always forming a circle in 3D space. In the other side, if we set the viewpoint from any point belonging to the rotation axis, we can see that the camera origin forms a spatial circle S around the point of view, as shown in Figure 3.7 (b). Therefore, we define point on rotation axis as the center of that spatial circle S . Besides, the position relationship between the rotation axis and the camera position is constant during the motion.

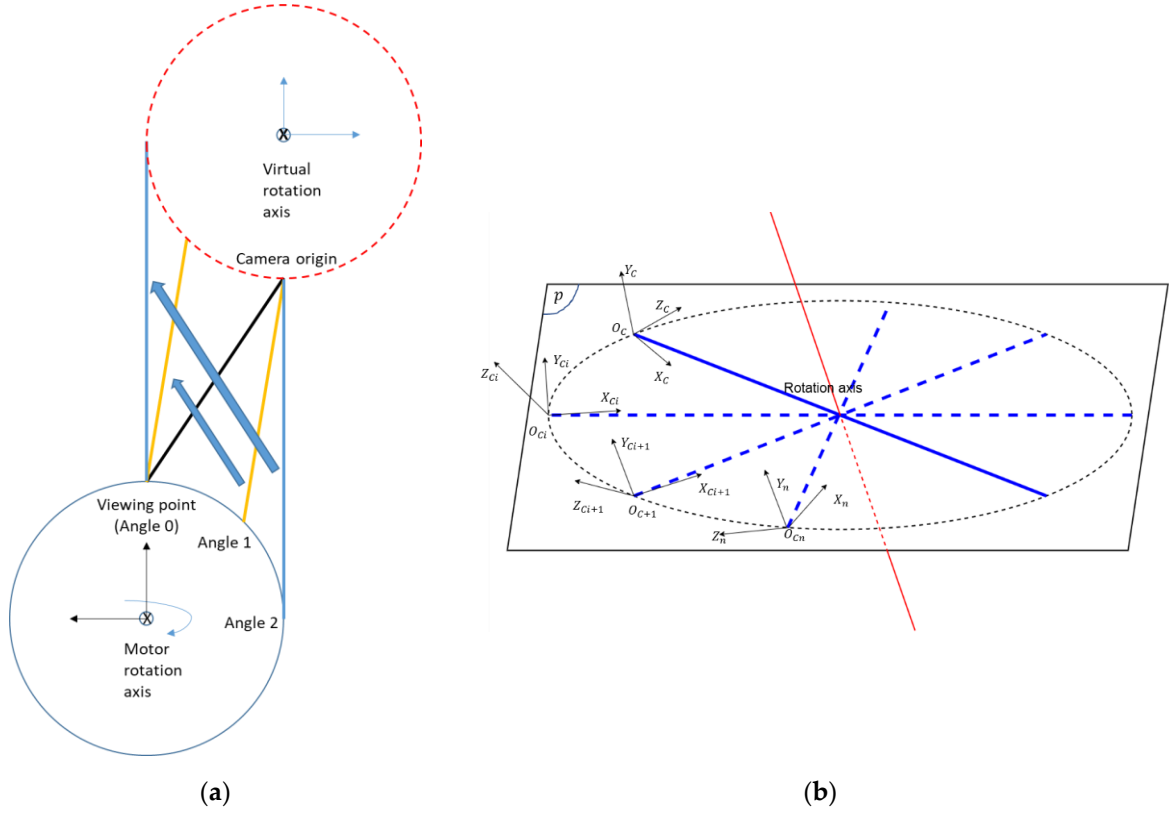


Figure 3.7. a) Virtual rotation axis defines; b) Camera coordinate systems at different times with the point of view is lie in the rotation axis.

Define C as a point on rotation axis mentioned above, using C , we can transform any 3D point in the camera coordinate system at any angular position ϕ to the predefined camera coordinate system (absolute coordinate system). Here, we choose the angular position at which the system begins to move as an absolute coordinate system ($\phi=0$).

From here, we define A_B^F as the coordinate of A_B in the coordinate system F , and R_ϕ as the rotation matrix that rotate a ϕ degree from M_0 to M_ϕ . Suppose we obtain two frames M_0 and M_ϕ during the motion of the motor, as shown in figure 3.8. M_0 is the starting frame and is also defined as the absolute coordinate system. M_ϕ is the frame we obtain after the motor rotated ϕ degree. We proposed a process to convert the coordinate of any point in the M_ϕ coordinate system to the absolute coordinate system M_0 . Suppose we have a laser point A in the coordinate system M_ϕ , lets notate it as A^ϕ . Here we need to determine the coordinate of point A in the absolute coordinate system M_0 . Call A' is a virtual point of A satisfies (12). On the other hand, C is the point on rotation axis. By applying vector math for vector v_3 , we can say that v_3 satisfies (13). Call R_ϕ is the rotation matrix that rotates frame M_0 to M_ϕ a ϕ degree. We can describe the relationship between v_5 and t as (14). From the two-relationship shown in (12) and (14), we can be easy to get (15). By applying vector math again, we can get (16). Finally, the coordinate of the laser point A in the camera coordinate system M_ϕ be rewritten like (17) in the absolute coordinate system M_0 .

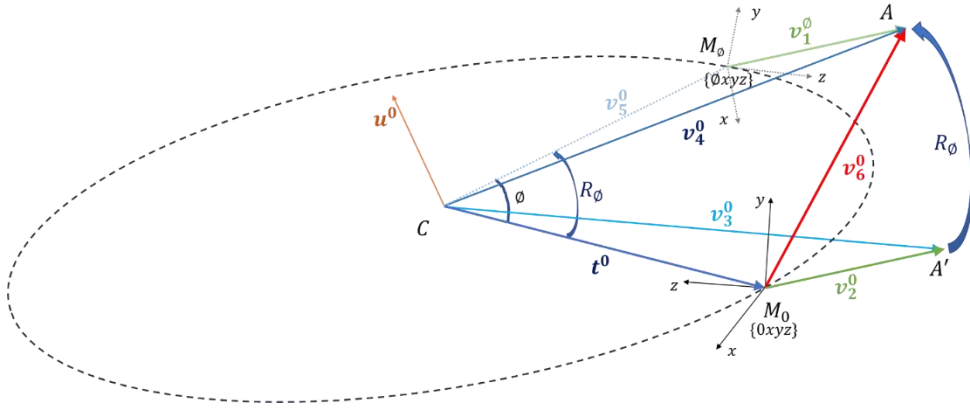


Figure 3.8. Relationship between the laser point in the corresponding coordinate system to the absolute coordinate system.

$$v_2^0 = v_1^\phi \quad (12)$$

$$v_3^0 = v_2^0 + t^0 \quad (13)$$

$$v_5^0 = R_\phi t^0 \quad (14)$$

$$v_4^0 = R_\phi v_3^0 \quad (15)$$

$$v_6^0 = v_4^0 - t^0 \quad (16)$$

$$v_6^0 = R_\phi(v_2^0 + t^0) - t^0 \quad (17)$$

In summary, the 3D transformation relationship between point A in any coordinate system M_ϕ to the absolute coordinate system M_0 has three processes: translation using translation matrix t^0 from any coordinate system M_ϕ to a coordinate system with the origin at the point in the rotation axis C , the process of rotating the vector v_3^0 by a corresponding angle using rotation matrix R_ϕ , here we call it v_4^0 , and the process of the inverse translating the vector v_4^0 from C to the origin of the absolute coordinate system.

$$A^0 = R_\phi(A^\phi + t^0) - t^0 \quad (18)$$

During the motion, we will obtain a sequence of consecutive frames, using the conversion of all pixels in the current coordinate systems to a destination coordinate system shown in the expression (18), and combining all the results, we can get the reconstruction of the 3D scanned scene.

In expression (18), we have 9 hidden components in the rotation matrix R and 3 other hidden components in the rotation matrix R . Therefore, we need to specify 12 variables. Re-representing the above equation is necessary to reduce the complexity of expression. On the other hand, the rotation matrix around any axis u is defined as (19). The specific interpretation has been defined as [32]. By replacing the expression matrix rotation (19) to the above expression. Our transformation expression has only 7 unknowns, where 3 are the coordinates

of the center of rotation, 3 are the coordinates of the axis vector, and the remaining unknown is the known rotation angle.

$$R_{u,\phi} = \begin{bmatrix} \cos\phi + u_x^2(1 - \cos\phi) & u_x u_y(1 - \cos\phi) - u_z \sin\phi & u_x u_z(1 - \cos\phi) + u_y \sin\phi \\ u_x u_y(1 - \cos\phi) + u_z \sin\phi & \cos\phi + u_y^2(1 - \cos\phi) & u_y u_z(1 - \cos\phi) - u_x \sin\phi \\ u_z u_x(1 - \cos\phi) + u_y \sin\phi & u_z u_y(1 - \cos\phi) + u_x \sin\phi & \cos\phi + u_z^2(1 - \cos\phi) \end{bmatrix} \quad (19)$$

Camera-motor calibration

During the rotation axis calibration as well as the scanning process, our system rotates at a fixed angle every step. During calibration, for each angle θ , the camera acquires an image that contains the calibration board. During the calibration process, the camera does not move, and the calibration board will be fixed on the turntable which will rotate with the motor's motion. Set the viewing point at the origin of the calibration board coordinate system, we can see that the camera coordinate system moves in a circular motion.

Determine the origin of the camera coordinates system in the calibration board

After the camera calibration, for each camera position, the transformation matrix consisting of the rotation matrix R_C and the translation matrix T_C can be determined through the calibration board image which will satisfy [18]:

$$X^C = R_C X^W + T_C \quad (20)$$

The optical center of the camera is the origin of the camera coordinate system, so the origin coordinate of the camera coordinate system is $(0,0,0)^T$. From the above expression, with R_C and T_C known in advance, we can easily determine the coordinates X^W of the camera optical center in the calibration board coordinate system:

$$X^W = -R_C^{-1} T_C \quad (21)$$

Each calibration board image gives us coordinates of the camera optical center at each motor angular position, the set of all these points $c = \{O_C, O_{C1}, \dots, O_{Cn}\}$ is an arc in spatial, as shown in Figure.

Determine the orientation vector in the coordinate system of the calibration board

After determining all the coordinates of the camera optical center at every angle of the motor, using the least-square method, we can estimate the plane p containing the set of points according to (12).

The perpendicular bisector of a line segment formed from any two points on an arc always passes through its center. Therefore, the intersection of two orthogonal formed from any 4 points on the circle always intersects at the center of the circle (illustration). In other words, from any set of points on a given circle, we can always determine the center of the circle. Any line in three-dimensional space has infinitely many orthogonal lying on the orthogonal plane, so we need to determine the orthogonal containing the center of the circle. The orthogonal here

is defined as the line of intersection between the perpendicular bisector of the line segment and the plane containing the arc.

$$p: Ax + By + Cz + D = 0 \quad (22)$$

Considering the line segment formed by any two points O_i and O_{i+1} lying on the arc. The perpendicular plane is determined as follows: the normal vector is defined as the vector n_i , and the point in the plane is the midpoint K_i of the segment straight O_iO_{i+1} . Determine the set $\{k\}$ of orthogonal planes of the points on the arc by randomly choosing two points from the set of points lying on the arc.

Corresponding to each orthogonal plane belonging to the set of orthogonal planes $\{k\}$ and the plane containing the interior arc p , we can determine a corresponding median line. Repeating the above steps, we obtain the set of median lines $\{m\}$.

As shown in Figure 2.7 (b), considering any two orthogonal belonging to the set of median lines $\{m\}$, the two median lines always intersect at the circle center. Repeating the above steps, we obtain a set of points that are the rotation center $\{c\}$ of the circle. The coordinate of center point is determined as the average coordinates of all points in the center C of the circle after filtering noise in $\{c\}$.

Determine the orientation vector in the camera coordinate system

The rotation axis u and point on rotation axis C coordinates in the previous part are defined for the calibration board coordinate system. This coordinate system changes depending on the position of the calibration board, so it cannot be used for reconstruction during scanning. We need to use the rotation information in the camera coordinate system because the relationship between them is constant. Using the transformation relationship between the two coordinate systems shown in (20), we convert the plane p from the calibration board coordinate system to the camera coordinate system, then get its normal vector as the rotation vector. The point on rotation axis is also obtained in the same way.

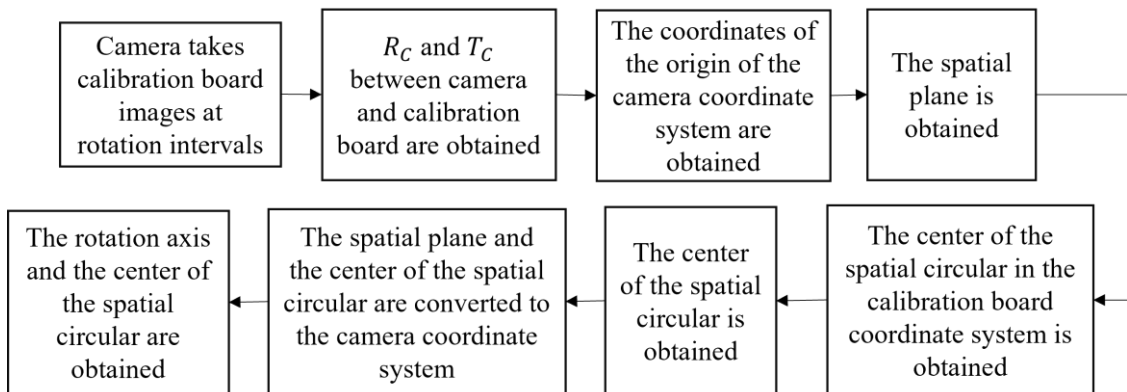


Figure 3.9. Pipeline of the camera-motor rotation axis calibration process.

The pipeline of the rotation axis calibration is shown in Figure 3.9. The camera takes the images of the calibration board at every angle of the motor. Using the camera calibration

parameters, the rotation R_C and the translation T_C matrix of each pose is specified. Then we can obtain the coordinates of the origin of the camera coordinate system in the calibration board coordinate system. By fitting them into a plane and using the transformation relationship between the calibration board coordinate system and the camera coordinate system, the rotation axis of the motor is obtained. The point on rotation axis known as center of the space circle obtained by using the geometry relationship. Then we can define the rotation information by the rotation vector u and the point in rotation axis C . Combined with the rotation angle, the rotation and translation matrix between the camera coordinate system and the absolute coordinate system can be obtained.

3.4. 3D surface reconstruction

After performing the calibration process, we can obtain the intrinsic parameters, the laser plane equation, the rotation axis, and the point belonging to rotation axis in the camera coordinate system. What we need to do now is to use these parameters to complete the reconstruction process. As mentioned before, the 3D surface reconstruction consists of 2 steps: data collection and reprocessing, and data processing. The data collection step is the step that the camera acquires the image, extract the laser stripe and convert them to into camera coordinates system. This step also gets the rotated angle and calculate the rotation matrix. The second step will use this information to estimate the depth of the laser stripe and save them to the program memory.

3.4.1. Introduction [6]

A digital 3D model is a numerical representation of a real object. Applications based on the 3D model are today growing more and more popular due to the increasing availability of 3D graphic devices and the decreasing cost of the computational power.

Scanning is a process that allows obtaining the 3D model in a fully automatic or semi-automatic way by measuring the geometric features of the object and then, the surface digital model represents the measured data. A scanning system is a device serving for conversion of a real object into digital 3D model. The scanned data is called point cloud data, this means each scanned points has a position in space in terms of a coordination system. 3D scanning systems can be divided based on the method of scanning or the device it used, such as structured light [4], line laser [13], etc.

3.4.2. Data collection and preprocessing

Assume that we have collected points pl of a single laser stripe. Call the laser plane equation is found as equation (6). As shown in Figure 3.10, we can see that each object point is the result of the intersection between laser plane and camera ray. Consider each laser point pl_i and the laser plane equation in the camera coordinate system, we can easily find the object point coordinate as equation (4) and (5). Repeating the above step for every laser point, we can have a set of laser stripe in the camera coordinate system, as shown in Figure 3.10.

By the time the motor rotating, each laser stripe corresponding with each motor angle, or rotation matrix, can be determined by its rotation axis which is found from the motor-camera calibration process. Because the camera and motor position are not change, so we do not need to modify the point on rotation axis during the scanning process. The rotation matrix can be calculated following the equation (19).

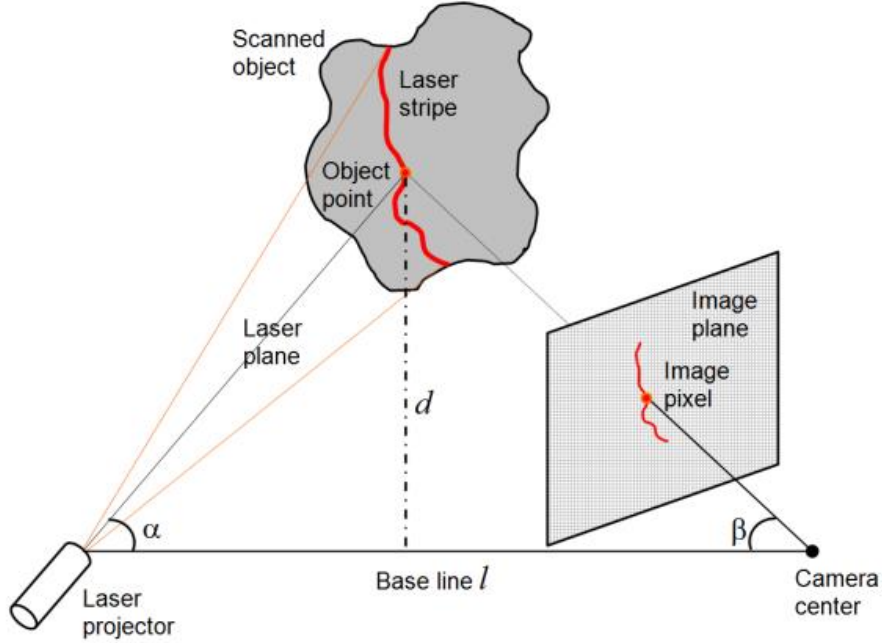


Figure 3.10. Triangulation based laser camera scanning [6].

3.4.3. Merging the point cloud dataset into a single point cloud

After performing the data collection and preprocessing, we have a collection of laser profile at each motor angle and its corresponding rotation matrix. This laser profile collection will be brought to common world coordinates system using the camera-motor calibration parameters. A single point cloud of the complete surface of the object will be then reconstructed.

To merge the obtained laser profile into a complete point cloud, all the points of these laser point data sets should be transformed into an absolute coordinate system. The absolute coordinate system (ACS) has one axis coincided with the rotation axis, which is obtained in the calibration step, as shown in Figure 3.7 (a). Let p_i be a point in a laser stripe of the camera coordinate system when the motor rotated with a rotation angle ϕ . This point in the camera coordinate system can be transformed to the ACS as follow:

$$p_i^{ACS} = R_{u,\phi}(p_i + T) - T \quad (23)$$

With $R_{u,\phi}$ is the transformation matrix performed the rotation transformation between the coordinate system and the WCS, which can be calculated as equation (23).

And the transformation matrix T performed the translation of the camera origin to the ACS origin can be seen as the point on rotation axis coordinate which is obtained in the calibration step. Figure 3.11 is an example of the transformation process. In Figure 3.11 (a), the laser profile of all the laser stripe is in laser plane, which is the plane we obtained from the calibration process. The corresponding result after transformation process is shown in the Figure 3.11 (b), which is each laser stripe rotated a corresponding angle.

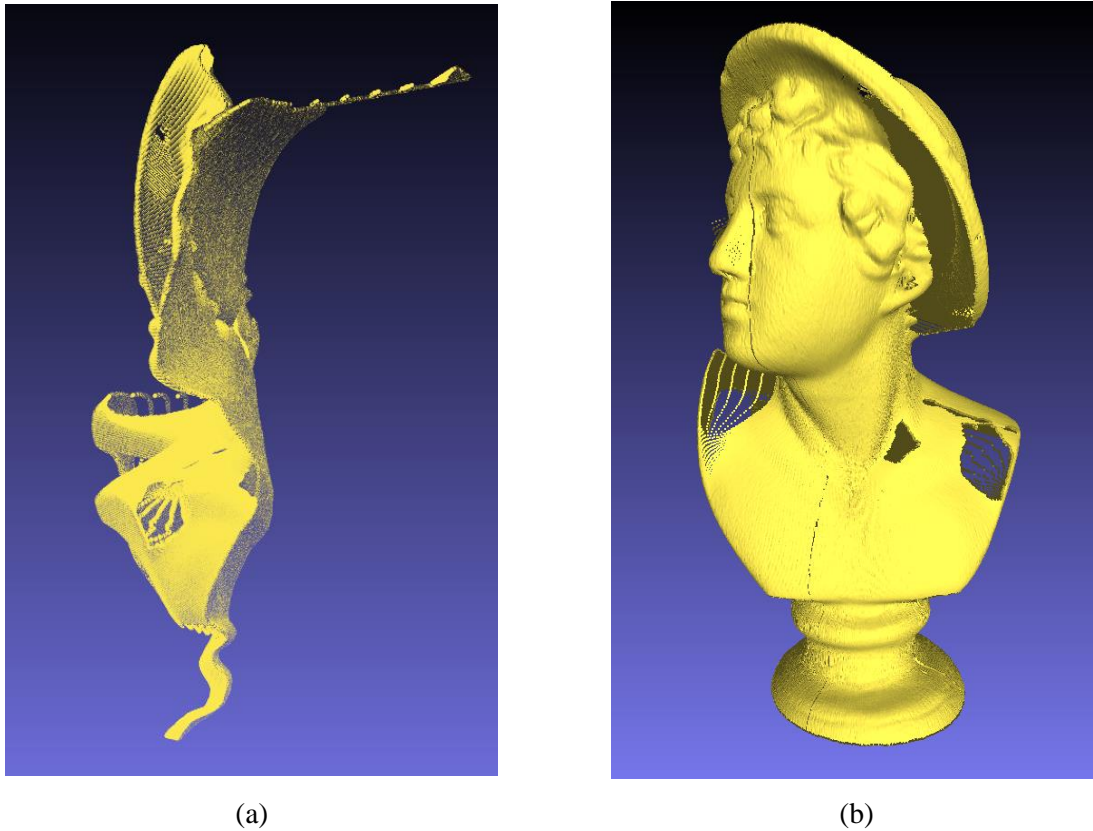


Figure 3.11. (a) Laser profile without transformation to ACS; (b) Laser profile after transform to ACS.

3.4.4. Removing noise and background

During the motor motion, camera may see some unwanted laser stripe or noise. As illustrate in Figure 3.12 (a), and (b). The laser stripe in the background is the unwanted noise which will cause error in result. Figure 3.12 (c) is the scanning result which is including the unwanted laser stripe. Because the laser stripe is not change during motor motion, therefore, it rotates around rotation axis and from a cylinder shape in the scanning result. Figure 3.12 (d) is the scanning result with the noise from scene, which is some brighter than laser point may be appear in the camera field of view. These noises also do not change during the rotation and perform a different spatial circle in the scanning result. These kinds of noise have to be removed to get the better scanning result.

To solve this problem, we apply two methods. To solve the noise from scene, we use the region of interest of image. The region of interest (ROI) of image is the area that contain only scanning object. In the finding laser strip from image processing, the finding laser algorithm

will always be performed within the ROI, which do not consider the noise's contain area. As shown in Figure 3.13 (a), ROI is the area within the red rectangle.

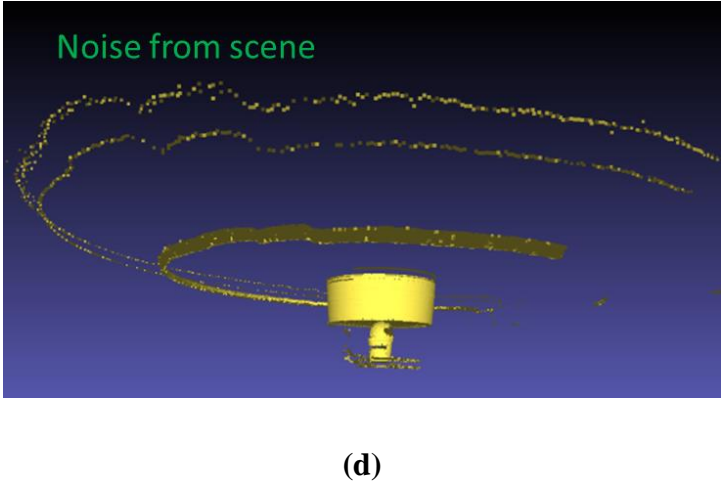
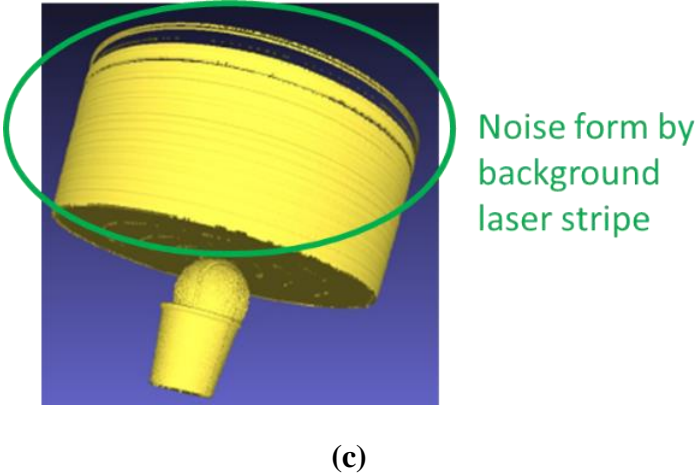
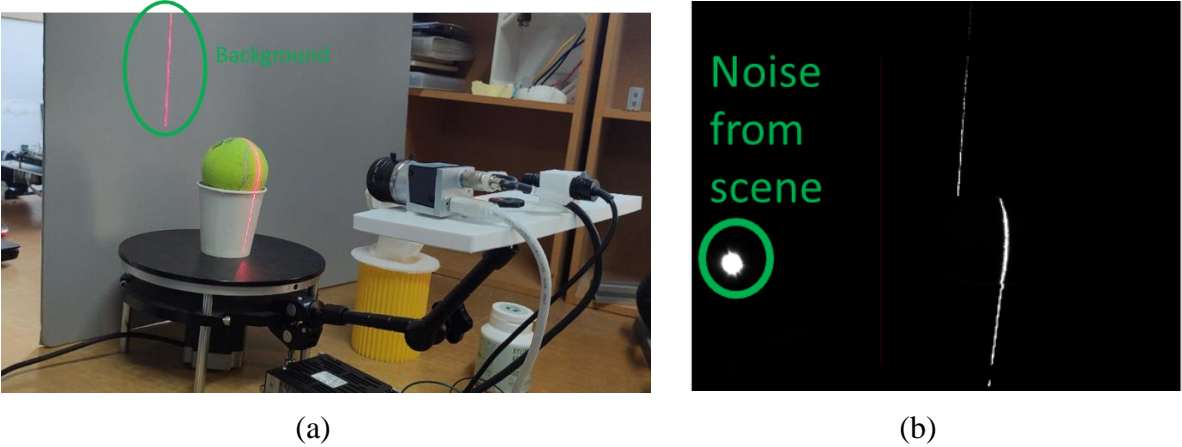


Figure 3.12. (a) Concept of scenery background; (b) Noise from scene; (c) Scanning result with noise from background in (a); (d) Scanning result after removing noise; (e) Scanning result with noise from scene in (b).

In order to remove the unwanted laser stripe, which is the area that laser stripe light up outside the scanning object, we use the distance of interest method. As shown in Figure 3.13 b, it is easy to define the distance of interest which is the gap that the laser point will be in. We will define all the bright point outside this gap as the noise.

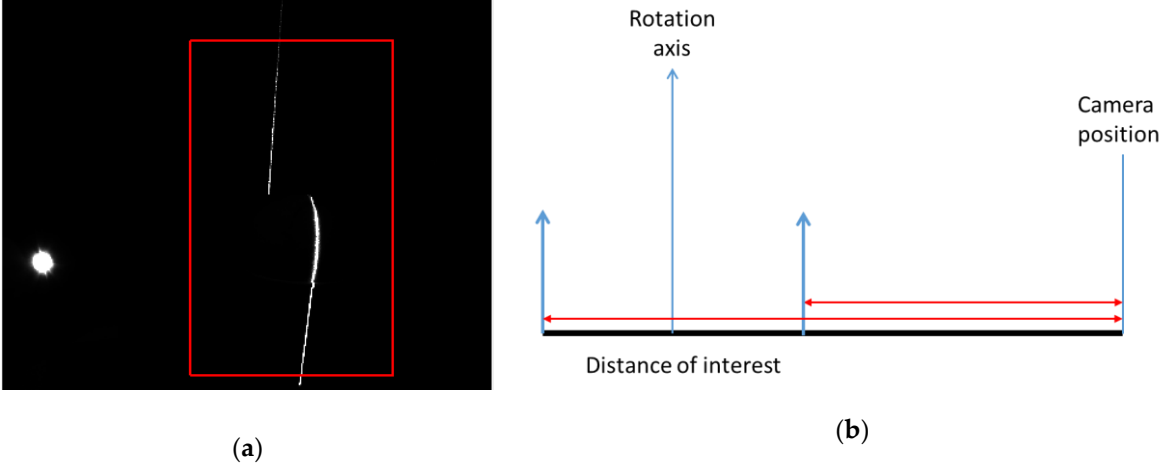


Figure 3.13. (a) ROI method for removing noise from the scene; (b) Distance of interest method to remove unwanted laser stripe.

The efficiency of the two methods is applied to our system with the good result. As shown in Figure 3.14, all the noise and unwanted laser stripe are completely removed, compared to the scanning result in Figure 3.12 (c) and (d).

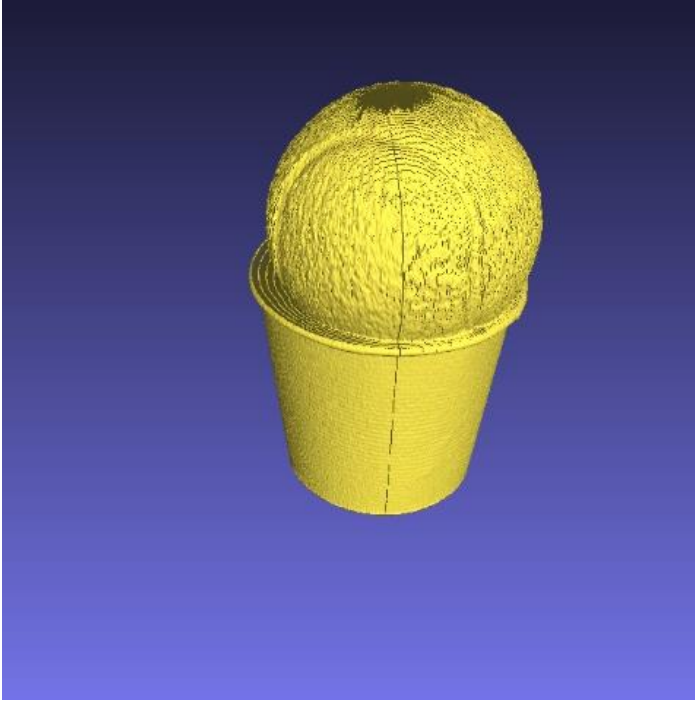


Figure 3.14. Scanning result after removing noise.

4. Experiments and results

The designer of the 3D scanner is shown in Figure 4.1 (a), and (b). The system is very simple and easy to assembly. The purpose of the calibration process is to obtain the camera intrinsic, distortion coefficients, laser plane equation, and the transformation parameter between the camera and the motor. In other to verify the accuracy of the calibration, three experiments were performed. The purpose of the first experiment is to evaluate the planarity of the plane of the scanning result. The second one was executed to verify the accuracy of the dimension of the scanned result. The final experiment is performed to check the quality of the scanned results of various objects.

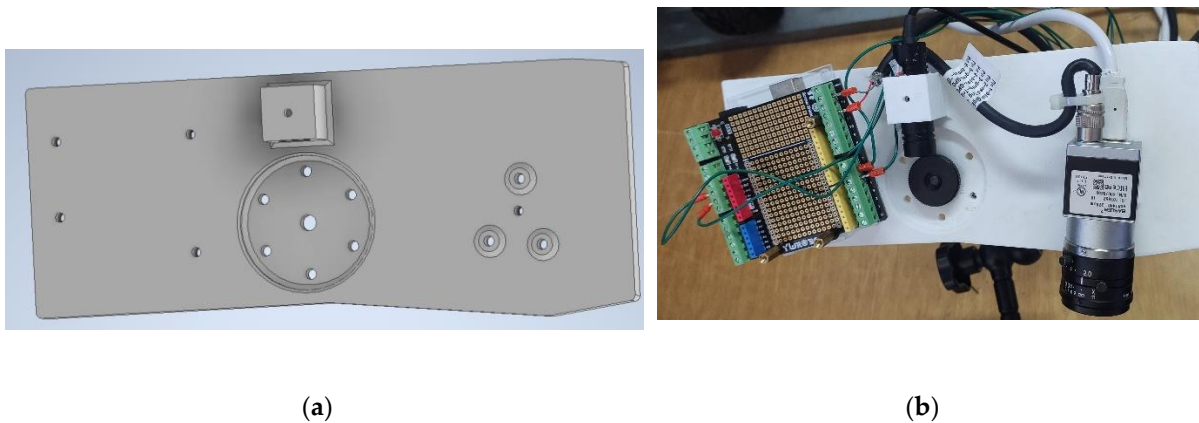


Figure 4.1. (a) The designing of camera-laser platform. (b) Camera-laser platform.

4.1. Calibration experiments

During the camera calibration, the calibration board was randomly placed in six different positions. Six corresponding images were captured by the camera that will be used to perform the camera calibration through OpenCV library.

During the camera-laser calibration, the calibration board was randomly placed in four positions. Two images were acquired for each pose, one contains the calibration board that is used for feature points, and another contains the laser line that is used to extract the laser line for laser plane fitting. The laser plane point is shown in Figure 4.2.

During the camera-motor calibration, the calibration board was placed in a fixed position, and the motor moved during the calibration. One image was acquired every time the motor finished a moving step. To reduce the error when we estimate the center points, we applied two filters. When we pick two points in the arc to obtain the perpendicular bisector, we choose only two points that its distance is more than 30 mm. When we calculate the intersection of two perpendicular bisectors, we also choose two perpendicular bisectors that its angular is more than 30 degrees. The arc points and its estimated center points was shown in figure 4.3 a. Figure 4.3 b shown the estimated center points.

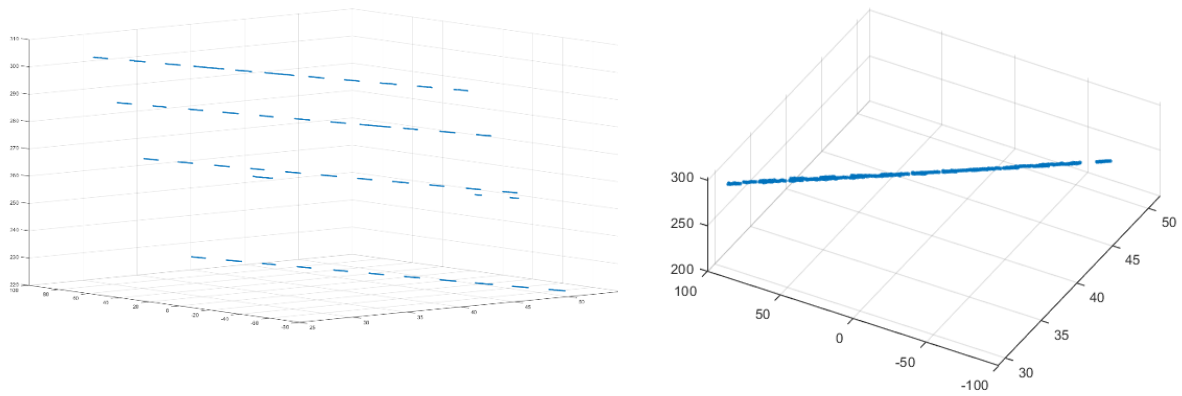


Figure 4.2. Laser plane in different viewpoint.

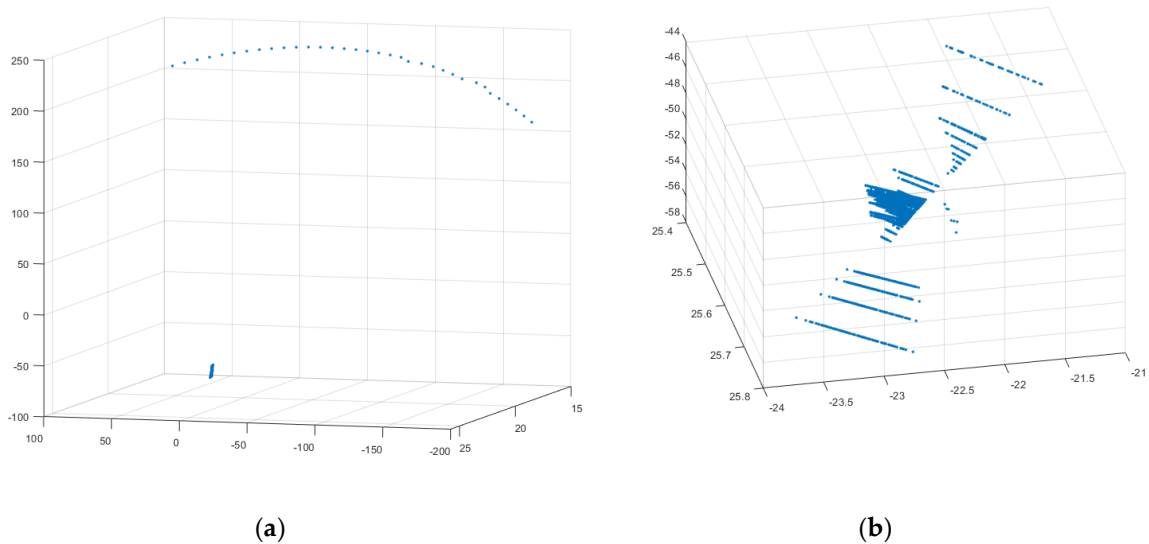


Figure 4.3. (a) The camera origin trajectory; (b) The camera origin trajectory and its estimated center points.

The calibration parameter of the camera and the laser plane is shown in the Table 1 and the rotation axis information are shown in the Table 2.

Table 1. Camera and camera-laser calibration results.

Parameter name	Value
Camera intrinsic matrix	$\begin{bmatrix} 1203.807 & 0 & 730.866 \\ 0 & 1202.398 & 590.244 \\ 0 & 0 & 1 \end{bmatrix}$
Distortion $k(1,2,3,4,5)$	-0.059; 0.112; 0.000; 0.002; -0.052
Laser plane equation	$-0.9887x - 0.0772y - 0.1285z + 74.2310 = 0$

Table 2. Camera-motor calibration results

Parameter name	Value
Rotation axis \mathbf{u}	$0.067, -0.996, -0.062$
Center points C	$36.762, -14.975, 277.383$

4.2. Result

4.2.1. Planarity of the plane

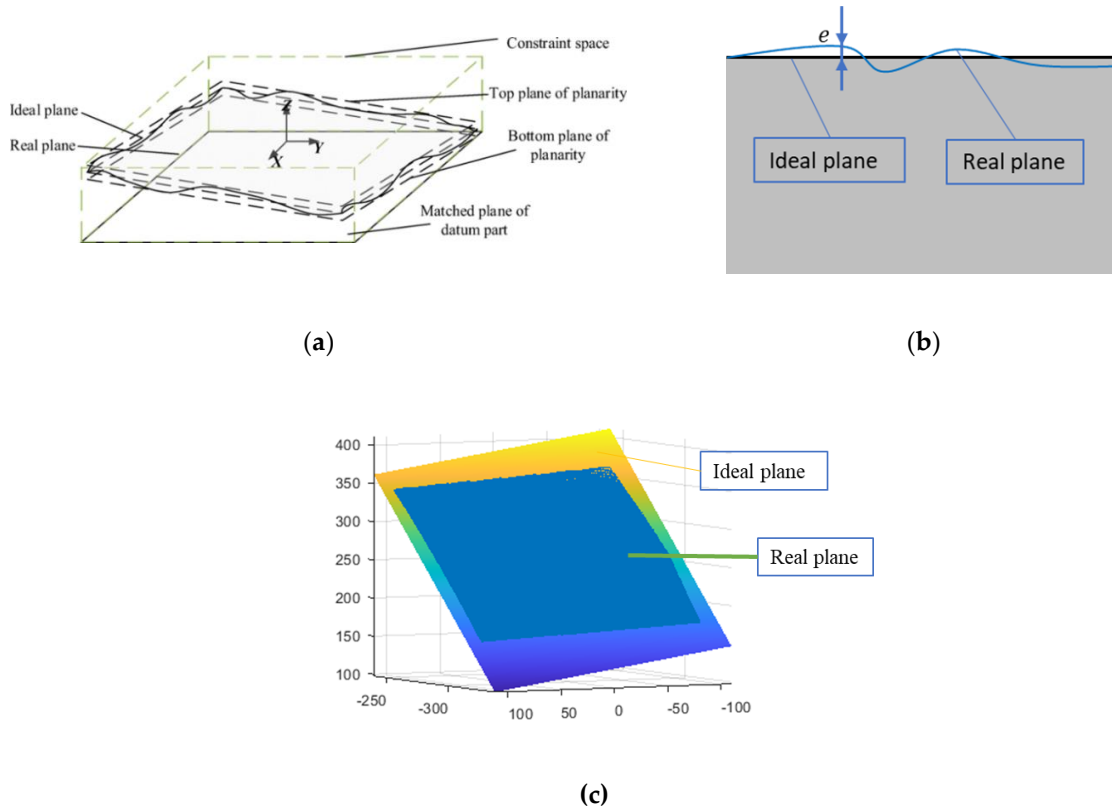


Figure 4.4. a) Definition of the plane constraints considering planarity [33]; b) Illustration of the ideal plane, real plane, and planarity of a plane; c) Result of our ideal plane and estimated plane.

We perform this experiment to evaluate the quality of the scanned surface. The definition of the plane constraints considering planarity [33] are shown in Figure 4.4 a). In our case, we use the information of the ideal plane and the real plane to measure and evaluate the planarity of the scanned plane.

In this experiment, the calibration board is used as the scanning object because of its flatness condition. Besides, we can use the feature points in the calibration board to define the reference coordinate system with respect to the camera coordinate system of the first frame. Because we defined the coordinate system of our scanning system as the coordinate system of the first

camera frame, it is easy to check the planarity of the plane. Therefore, we define the ideal plane as the plane of the feature points in the calibration board. The ideal plane obtained by using the perspective-n-point algorithm in the first frame of the camera. The real plane is the plane that is scanned by our scanning system. To determine the real plane, we must remove the outlier points in the scanning result using a point cloud tool, such as MeshLab, because it is not only having the calibration board in the scanning area. We calculated the distance from every estimated point to the ideal plane that is shown in Figure 4.4 b using (24). The parameter \mathbf{n} and \mathbf{q} are the ideal plane information, and the point \mathbf{p} is a point from the estimated point set.

$$e = \frac{|n^T(p - q)|}{\|n\|_2} \quad (24)$$

Figure 4.4 c is an example of the real plane that is scanned by our scanning system.

In this experiment, we used a calibration board as the scanning objects, as shown in Figure 4.5 (a). The scanned results of it are shown in Figure 4.5 (b). The average of the distance between the ideal plane and the points in the real plane are shown in Table 3.

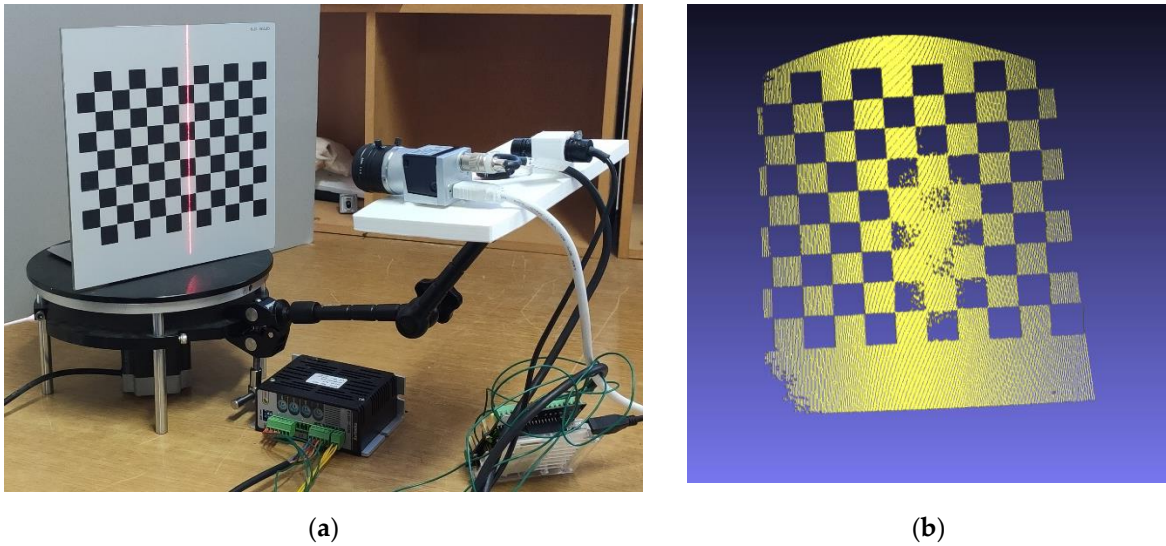


Figure 4.5. (a) Set up of experiment for planarity check; (b) Scanning result of the planarity check.

Table 3. Planarity result of the scanned calibration board

Number of tests	Planarity (mm)
1	0.3344
2	0.2933
3	0.36
4	0.2868
5	0.3499
6	0.3826
7	0.3384
8	0.396
9	0.3051
10	0.3215
11	0.3786
12	0.2845
13	0.3204
14	0.3001
15	0.4166

All the planarity errors are within the error range 0.5mm, which is acceptable for planarity of plane.

4.2.2. Accuracy check

To check the accuracy of the dimension of our scanning, one calibration block in Figure 4.6 (a) is used as the calibration object. The dimension of it is shown in Figure 4.6 (b). The scanned result of the calibration block is shown in Figure 4.6 (c).

The height difference of the calibration block is calculated using the 3D coordinate by our 3D reconstruction method to verify the error. We define the height difference of the calibration block as the distance between two surfaces or planes corresponding to it. Due to flatness issues, the two planes obtained from the scan result may not be parallel to each other. Therefore, we use the point-plane relationship to determine the distance between two planes as shown in figure 4.6 d. Assume we have two points set $Po1$ and $Po2$ corresponding to the 2 consecutive surfaces on the calibration block. From these 2 sets, using least square method, we can obtain the two planes $p1$ and $p2$ as shown in Figure Call $C1$ and $C2$ are the two corresponding centroids of the two-point sets $Po1$ and $Po2$. Then we calculate the projection point A of the centroid point $C1$ to plane $p1$, and the projection point B of the centroid point $C2$. We define the distance of the two planes as the average of the distance from point A to plane $p2$ and the distance from point B to plane $p1$.

$$d = \frac{d_1 + d_2}{2} \quad (25)$$

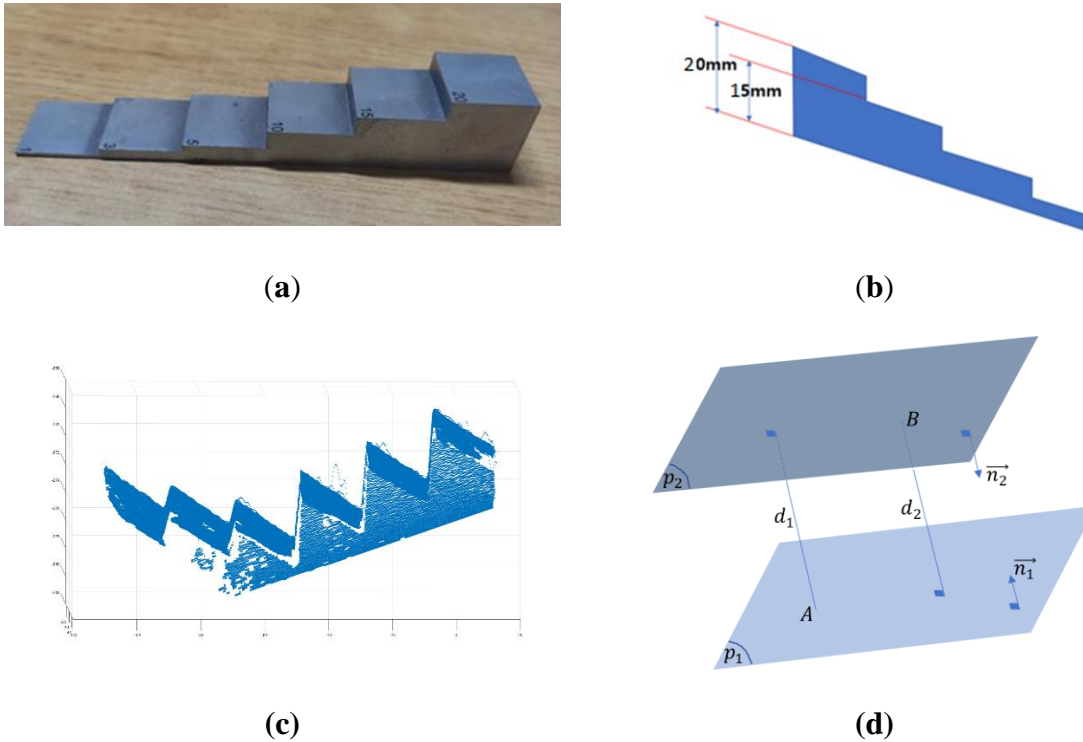


Figure 4.6. (a) Calibration block; (b) Dimension of the calibration block; (c) Scanned result of calibration block; (d) Illustration of the way to measure the distance between two planes.

Figure 4.7 is an example of a calibration block and its checking distance.

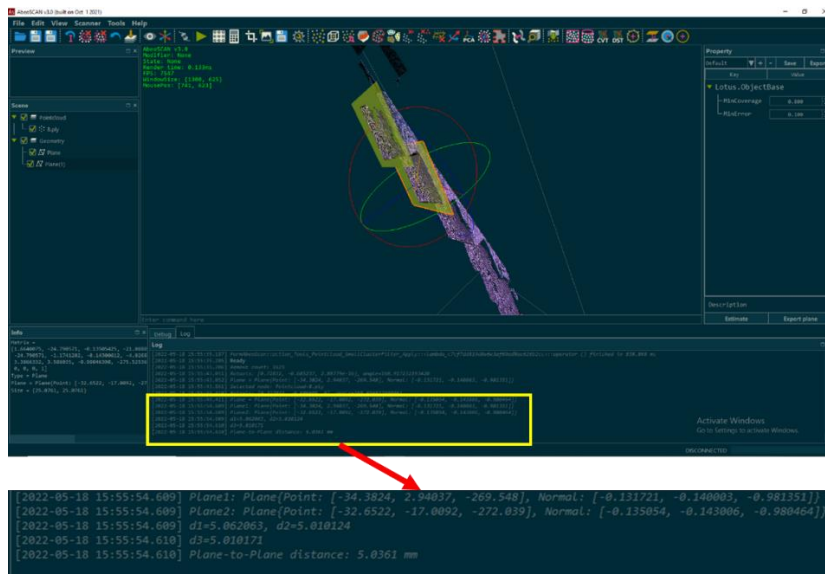


Figure 4.7. Two-planes distance checking with calibration block.

The average and the error of the distance between the two planes are shown in Table 4.

Table 4. The average and the error of the distance between the two planes of the calibration block with different scanning results.

Number of tests	Measured value (mm)	Real value (mm)	Error (mm)
1	4.9432	5	-0.0568
2	5.0505	5	0.0505
3	5.0094	5	0.0094
4	4.9890	5	-0.0110
5	5.0637	5	0.0637
6	5.0153	5	0.0153
7	5.0124	5	0.0124
8	5.0361	5	0.0361
9	5.0081	5	0.0081
10	5.001	5	0.0010
11	5.0407	5	0.0407
12	5.0134	5	0.0134
13	5.0241	5	0.0241
14	4.9915	5	-0.0085
15	5.0305	5	0.0305

All the measurements are within the error range of 0.07mm, and the average error is 0.01526mm. So, the 3D scan accuracy is acceptable.

4.2.3. Scanning quality check

This experiment is aimed at assessing the qualitative results regarding the reconstruction of scanning results of various shapes of objects. As shown in Figure 4.8, we scanned multiple items, such as a tennis ball and cup. Its results show that our scanner has a good scanning quality.



Figure 4.8. Scanning workspace for quality check and its scanning result.

Besides, we do one more experiment to scan the object with complicated features. Here we used a human statue as in Figure 4.9 (a). We also get a good result compared with the original object, as shown in Figure 4.9 (b).

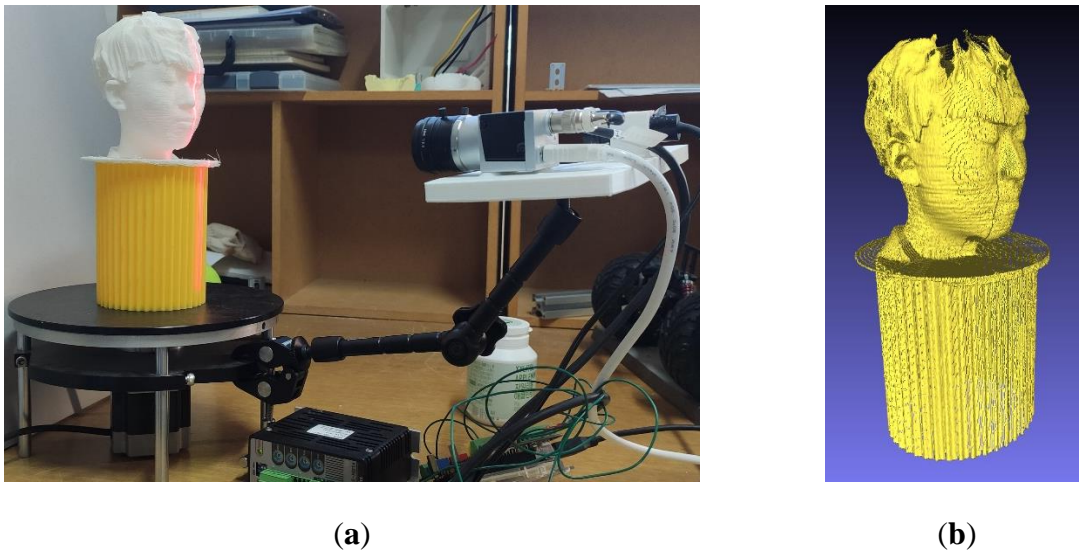


Figure 4.9. (a) Real human statue used for quality check; (b) Scanning result of the quality check.

5. Conclusion, limitation, and future work

In this study, a laser scanning system with a rotation axis was designed and calibrated to get the 3D data of a movable object. The study describes a step-by-step solution that can be easy to understand. It will give an overview of how to design a laser-based scanning system, which is now become popular and applicable in industries. Especially, a new calibration method for 1 axis rotating mechanism. The transformation information between any camera coordinate system and the absolute coordinate system should be determined for 3D reconstruction. Our calibration method can obtain the virtual rotation axis and its center point in the camera coordinate system. With the rotation axis and its center point, we can easily adjust the scanning resolution by adjusting the motor step angle. The calibration board image should cover all the image frame to archive good results.

In order to evaluate the calibration algorithm, we perform by checking the planarity, accuracy, and the depth information of the scanning objects. Using the scanning results of the calibration board surface and the calibration block, we proved that our algorithm has good accuracy. The laser scanning system for 3D point cloud data acquisition achieved high accuracy with the error ± 0.0637 mm. Moreover, the maximum object size can be adjusted by adjusting the distance between the camera and the motor position, as well as the camera lens and laser focus. Therefore, our scanning system is flexible with various sizes of scanned objects.

The limitation of this kind of scanner is that it is only applicable to movable reconstruction objects, and it can only scan objects that are within a fixed field of view of camera. With the proposed rotation axis calibration method. We can develop another scanner with rotation axis, in this case, the rotating part is the camera-laser platform. This kind of scanner is movable and can scan any fixed object.

Reference

1. Bellocchio, F.; Borghese, N.A.; Ferrari, S.; Piuri, V. *3D Surface Reconstruction: Multi-Scale Hierarchical Approaches*; 2012; Vol. 9781461456322; ISBN 1461456312.
2. Geiger, A.; Ziegler, J.; Stiller, C. StereoScan: Dense 3d Reconstruction in Real-Time. In Proceedings of the 2011 IEEE Intelligent Vehicles Symposium (IV); 2011; pp. 963–968.
3. Izadi, S.; Kim, D.; Hilliges, O.; Molyneaux, D.; Newcombe, R.; Kohli, P.; Shotton, J.; Hodges, S.; Freeman, D.; Davison, A.; et al. *KinectFusion: Real-Time 3D Reconstruction and Interaction Using a Moving Depth Camera*; 2011;
4. Moreno, D.; Taubin, G. Simple, Accurate, and Robust Projector-Camera Calibration. In Proceedings of the 2012 Second International Conference on 3D Imaging, Modeling, Processing, Visualization & Transmission; 2012; pp. 464–471.
5. Zhang, L.; Dong, H.; el Saddik, A. From 3D Sensing to Printing: A Survey. *ACM Transactions on Multimedia Computing, Communications and Applications* 2015, 12.
6. Nguyen, H.-C. Development of 3D Vision Systems Using Stereo-Camera and Laser-Vision for 3D Measurement, Inspection and Reconstruction 2016.
7. Roman, C.; Inglis, G.; Rutter, J. Application of Structured Light Imaging for High Resolution Mapping of Underwater Archaeological Sites. In Proceedings of the OCEANS'10 IEEE SYDNEY; 2010; pp. 1–9.
8. Fan, H.; Qi, L.; Ju, Y.; Dong, J.; Yu, H. Refractive Laser Triangulation and Photometric Stereo in Underwater Environment. *Optical Engineering* **2017**, 56, 1, doi:10.1117/1.OE.56.11.113101.
9. Gestel, N. van; Cuypers, S.; Bleys, P.; Kruth, J.P. A Performance Evaluation Test for Laser Line Scanners on CMMs. *Optics and Lasers in Engineering* **2007**, 47, 336–342.
10. Pawar, S.S.; Mithaiwala, H.; Gupta, A.; Jain, S. Review Paper on Design of 3D Scanner. In Proceedings of the IEEE International Conference on Innovative Mechanisms for Industry Applications, ICIMIA 2017 - Proceedings; Institute of Electrical and Electronics Engineers Inc., July 11 2017; pp. 650–652.
11. Nguyen, C.; Lee, B.-R. 3D Model Reconstruction System Development Based on Laser-Vision Technology. *International Journal of Automation Technology* **2016**, 10, 813–820, doi:10.20965/ijat.2016.p0813.
12. Cai, X.; Zhong, K.; Fu, Y.; Chen, J.; Liu, Y.; Huang, C. Calibration Method for the Rotating Axis in Panoramic 3D Shape Measurement Based on a Turntable. *Measurement Science and Technology* **2021**, 32, doi:10.1088/1361-6501/abcb7e.

13. Lee, J.; Shin, H.; Lee, S. Development of a Wide Area 3d Scanning System with a Rotating Line Laser. *Sensors* **2021**, *21*, doi:10.3390/s21113885.
14. Cai, H.; Song, Y.; Shi, Y.; Cao, Z.; Guo, Z.; Li, Z.; He, A. Flexible Multicamera Calibration Method with a Rotating Calibration Plate. *Optics Express* **2020**, *28*, 31397, doi:10.1364/oe.402761.
15. Bisogni, L.; Mollaiyan, R.; Pettinari, M.; Neri, P.; Gabiccini, M. Automatic Calibration of a Two-Axis Rotary Table for 3d Scanning Purposes. *Sensors (Switzerland)* **2020**, *20*, 1–21, doi:10.3390/s20247107.
16. Kurnianggoro, L.; Dung, H. van; Jo, K.-H. Calibration of a 2D Laser Scanner System and Rotating Platform Using a Point-Plane Constraint. *Computer Science and Information Systems* **2015**, *12*, 307–322, doi:10.2298/CSIS141020093K.
17. Niu, Z.; Liu, K.; Wang, Y.; Huang, S.; Deng, X.; Zhang, Z. Calibration Method for the Relative Orientation between the Rotation Axis and a Camera Using Constrained Global Optimization. *Measurement Science and Technology* **2017**, *28*, 055001, doi:10.1088/1361-6501/aa5fd4.
18. Zhu, Z.; Yang, J.; Wang, X.; Qi, G.; Wu, C.; Fan, H.; Qi, L.; Dong, J. Rotation Axis Calibration of Laser Line Rotating-Scan System for 3D Reconstruction. In Proceedings of the 2020 11th International Conference on Awareness Science and Technology (iCAST); 2020; pp. 1–5.
19. Cao, C.-T.; Do, V.-P.; Lee, B.-R. A Novel Indirect Calibration Approach for Robot Positioning Error Compensation Based on Neural Network and Hand-Eye Vision. *Applied sciences* **2019**, *9*, 1940, doi:10.3390/app9091940.
20. Dunin-barkovskii, I.I. Construction of System for Controlling the Dimensions of Large-Scale Parts Based on a 3D Machine Vision System. *Measurement Techniques* **2004**, *47*, 1168–1173, doi:https://doi.org/10.1007/s11018-005-0081-5.
21. Rovira-Más, F.; Zhang, Q.; Reid, J.F. Stereo Vision Three-Dimensional Terrain Maps for Precision Agriculture. *Computers and Electronics in Agriculture* **2008**, *60*, 133–143, doi:https://doi.org/10.1016/j.compag.2007.07.007.
22. Brown, R.G.; Chase, J.G.; Hann, C.E. A Pointwise Smooth Surface Stereo Reconstruction Algorithm without Correspondences. *Image and Vision Computing* **2012**, *30*, 619–629, doi:https://doi.org/10.1016/j.imavis.2012.06.003.
23. Fryer, J. *Lens Distortion for Close Range Photogrammetry*; 1986;
24. Brown, D. *Close-Range Camera Calibration*.; 1971.
25. Lanman, D.; Taubin, G. Build Your Own 3D Scanner: 3D Photography for Beginners. *ACM SIGGRAPH 2009 Courses, SIGGRAPH '09* **2009**, *8*, doi:10.1145/1667239.1667247.

26. Eberly, D. *Least Squares Fitting of Data by Linear or Quadratic Structures*;
27. Fisher, R.B.; Naidu, D.K. A Comparison of Algorithms for Subpixel Peak Detection. In *Image Technology*; Springer Berlin Heidelberg, 1996; pp. 385–404.
28. Blais, F.; Rioux, M. *REAL-TIME NUMERICAL PEAK DETECTOR*; 1986; Vol. 11;.
29. Hemayed, E.E. A Survey of Camera Self-Calibration. In Proceedings of the Proceedings - IEEE Conference on Advanced Video and Signal Based Surveillance, AVSS 2003; Institute of Electrical and Electronics Engineers Inc., 2003; pp. 351–357.
30. Zhang, Z. A Flexible New Technique for Camera Calibration. *IEEE Transactions on Pattern Analysis and Machine Intelligence* **2000**, *22*, 1330–1334, doi:10.1109/34.888718.
31. Usamentiaga, R.; Molleda, J.; Garcia, D.F. Structured-Light Sensor Using Two Laser Stripes for 3D Reconstruction without Vibrations. *Sensors (Switzerland)* **2014**, *14*, 20041–20063, doi:10.3390/s141120041.
32. Taylor, C.; Kriegman, D. Minimization on the Lie Group $SO(3)$ and Related Manifolds. **2001**.
33. Cui, Z.; Du, F. Assessment of Large-Scale Assembly Coordination Based on Pose Feasible Space. *International Journal of Advanced Manufacturing Technology* **2019**, *104*, 4465–4474, doi:10.1007/s00170-019-04307-8.